Hindawi
Geofluids
Volume 2019, Article ID 9732674, 26 pages
https://doi.org/10.1155/2019/9732674

Research Article

Geochemistry and Genesis of Oil and Gas Seeps in the Junggar Basin, NW China: Implications for Hybrid Petroleum Systems

Jingkun Zhang,[1] Jian Cao,[1] Yan Wang,[1] Jun Li,[2] Guang Hu,[3] Ni Zhou,[4] and Tianming Shi[4]

[1]*MOE Key Laboratory of Surficial Geochemistry, Department of Earth and Planetary Sciences, Nanjing University, Nanjing, Jiangsu 210023, China*
[2]*Department of Exploration, PetroChina Xinjiang Oilfield Company, Karamay, 834000 Xinjiang, China*
[3]*State Key Laboratory of Oil and Gas Reservoir Geology and Exploitation, School of Earth Science and Technology, Southwest Petroleum University, Chengdu, Sichuan 610059, China*
[4]*Research Institute of Experiment and Testing, PetroChina Xinjiang Oilfield Company, Karamay, 834000 Xinjiang, China*

Correspondence should be addressed to Jian Cao; jcao@nju.edu.cn

Received 20 February 2019; Revised 5 June 2019; Accepted 12 June 2019; Published 1 August 2019

Academic Editor: Ricardo L. Silva

The Junggar Basin of NW China is representative in containing oil and gas seeps worldwide as there are a wide variety of oil and gas seeps over a large area. However, the genesis of these seeps remains poorly known, limiting the understanding of their implications for petroluem geology and hydrocarbon exploration. Here, we investigate 26 samples of oil and gas seeps from nine outcrops within five areas along the margins of the Junggar Basin to determine the geochemical characteristics of the hydrocarbons, constrain their genesis, and discuss future exploration strategies. Results indicate one type of gas seeps and five types of oil seeps. The gas seeps are derived from low-maturity Jurassic source rocks and occur in the Wusu and Dushanzi areas in the western segment of the southern basin. Type 1 oil seeps, sourced from lower Permian rocks (P_1f), occur on the northwestern margin. Type 2 oil seeps, derived from middle Permian source rocks (P_2l/P_2p), occur on the eastern segment of the southern margin and eastern margin of the Junggar Basin. Type 3 oil seeps, with Jurassic source rocks, occur in the Qigu area in the middle segment of the southern basin. Type 4 oil seeps, with Cretaceous source rocks, occur in the Anjihai and Huoerguosi areas within the middle segment of the southern basin. Type 5 oil seeps mainly have Paleogene source rocks with a minor contribution from Jurassic rocks and occur in the Wusu and Dushanzi areas in the western segment of the southern basin with the single-type gas seeps. These results indicate the presence of lacustrine hybrid petroleum systems within the Junggar Basin with complex oil and gas sources and migration-accumulation. Six potential areas along the basin margin were proposed for exploration in the future.

1. Introduction

Oil and gas seeps represent the surface escapes of subsurface hydrocarbon accumulation, and thus, the presence of oil and gas seeps provides indirect information on deeper subsurface deposits of hydrocarbons that can potentially aid exploration [1, 2]. As refinement of exploration models yields economic benefits, oil and gas seeps globally have been the subject of in-depth studies [3–7].

The Junggar Basin is a large superimposed and petroliferous basin in NW China within which oil and gas seeps are widely distributed on the basin margins [8, 9]. The basin is well known and representative in containing oil and gas seeps worldwide due to the large variety and wide occurrence and thus provides an ideal target for the study of oil and gas seeps [10]. Early investigations by the Xinjiang Oilfield Company produced two internal technical reports: "The Distribution Rules of Oil–Gas Seeps in the Junggar Basin" [11] and Oil–Gas Seeps Field Survey PetroChina Xinjiang Oilfield Company [12]. Results show that more than 200 hydrocarbon seeps have been found in the basin. However, technological limitations initially restricted research to establishing the basic geochemical characteristics of the oil and gas seeps, and it was not until the 1980s that more detailed studies were published [13, 14]. Recent research concerning oil and gas seeps has focused mainly on mud volcanoes in the southern

basin, as mud volcanoes typify the occurrences of oil and gas seeps within the basin [15–20]. However, there are relatively few studies for the other diverse oil and gas seeps. As such, the genesis of these seeps in a basin scale remains poorly known, limiting the understanding of their presence to petroleum geology and hydrocarbon exploration.

The present study presents geochemical data from 26 oil and gas seep samples from nine outcrops within the Junggar Basin, with the aim to improve the understanding of the formation and indication for the exploration of the oil and gas seeps in the basin. The geochemical data provide important information concerning the genesis of the seeps, the geochemical characteristics of their source rocks, and the secondary processes of alteration within petroleum systems, which may serve as a reference for future research and advance exploration for hydrocarbons in the region. The results can also be referred to as representatives of oil and gas geochemistry and accumulation with secondary alteration worldwide.

2. Geological Setting

The Junggar Basin is located in the northern Xinjiang Uygur Autonomous Region of NW China (Figure 1(a)) and is one of the many petroliferous basins within central Asia and part of the Circum-Tibetan Plateau Basin-Range System [21, 22]. It has a roughly triangular shape and is bordered by the Tianshan Mountains to the south, the Altai Mountains to the NE, and the West Junggar Mountains to the NW (Figure 1(b)). This basin is a polycyclic superimposed basin that developed on the Junggar Terrane and occurs at a convergent boundary between the Kazakhstan, Siberia, and Tarim plates [23, 24]. The tectonic evolution of the Junggar Basin is subjected to late Paleozoic–Cenozoic and can be divided into four main stages: (1) development of a late Carboniferous–early Permian foreland oceanic basin, which evolved into (2) a middle–late Permian intracratonic foreland basin, (3) development of a Triassic–Cretaceous inland depression, and finally, (4) Paleogene–Quaternary reactivation of the foreland basin [9]. Rock strata in the basin were deposited between the Paleozoic and the Cenozoic and contain six possible hydrocarbon sources of Carboniferous, Permian, Triassic, Jurassic, Cretaceous, and Paleogene age. These source rocks form the resource foundation for the hybrid petroleum systems of the basin (Figure 2; [25]). Figure 2 shows composite source–reservoir–caprock assemblages within the entire Junggar Basin, indicative of the hybrid petroleum systems. The hydrocarbon seeps dominantly occur within orogenic belts on the margins of the basin where Mesozoic and Cenozoic strata are exposed (Figure 1; Table 1).

3. Samples and Methods

3.1. Samples. Based on the spatial distribution within the Junggar Basin, the oil and gas seeps are divided into five regions: northwestern margin (NW), western segment of the southern margin (SW), middle segment of the southern margin (SM), and eastern segment of the southern margin (SE) and eastern margin (E; Figure 1, Table 1). The 26 oil-gas seep samples collected from nine outcrops within the five regions are representative of the entire Junggar Basin, as inferred from the following three factors: (i) the sample localities are widely distributed around the entire basin margin (Figure 1), (ii) the strata from which samples were collected cover largely from the Paleozoic to the Mesozoic (Figure 2; Table 1), and (iii) the sampled material covers all the oil and gas seep types, including 14 oil sands (Figure 3(a)), 3 pure bitumens (Figure 3(b)), 6 crude-oil seeps (Figures 3(c) and 3(d)), and 3 gas seeps (Figures 3(e) and 3(f)).

3.2. Methods. Twenty-five samples of solid materials including 14 oil sands, 3 bitumens, and 8 source rocks were crushed to powder (<100 mesh) and then treated for 72 hours using a Soxhlet apparatus with a solvent mixture of dichloromethane and methanol (93 : 7). The extracted material (e.g., bitumen), 6 crude oils from well, and 6 crude-oil seeps from outcrops were mixed with *n*-hexane and allowed to stand for 12 hours, yielding asphaltene. These residual extracts and crude oils were then fractionated using open silica-gel column chromatography. The sequence of solvents used was *n*-hexane, a mixture of *n*-hexane and dichloromethane (2 : 1), and finally, methanol. These steps produced saturated hydrocarbons, aromatic hydrocarbons, and resins, respectively.

Carbon isotope compositions of extracted bitumen components and oils were determined using a MAT 253 mass spectrometer. The instrument precision was better than 0.1‰, and isotopic ratios are reported in standard δ notation relative to the Vienna Peedee Belemnite (VPDB) standard.

The saturated hydrocarbons of bitumen extracts and oils were analyzed for molecular characteristics using gas chromatography and gas chromatography–mass spectrometry (GC–MS). The analysis used a HP6890 gas chromatograph with an HP-5 column (30 m × 0.32 mm i.d.) and a film thickness of 0.25 μm. Nitrogen was employed as a carrier gas. The GC oven temperature was initially held at 80°C for 5 min, heated from 80°C to 290°C using a 4°C/min ramp, and then held at this temperature for 30 min. The GC–MS analyses were conducted using an Agilent 5973I mass spectrometer interfaced with a HP6890 gas chromatograph and fitted with the same type of column as that used for GC analyses. Helium was employed as a carrier gas. The GC oven temperature for the GC–MS analysis was initially held at 60°C for 5 minutes, increased to 120°C using a ramp of 8°C/min, increased again from 120°C to 290°C using a ramp of 2°C/min, and finally, held at 290°C for 30 min.

For the collection of three gas mud-volcano samples, a glass container was put into the muddy water and above the gas vent (bubbles in the muddy water) after the air in the container was removed completely. After the gas bubbles appear, let the gas flow into the container as much as possible to get the gas samples. In addition, some gas is dissolved in the water. Thus, it is possible to get small amount of gas samples by extracting the gas in the muddy water samples [15].

The carbon isotopic compositions of the three gas seep samples were determined using an Optima isotope ratio mass

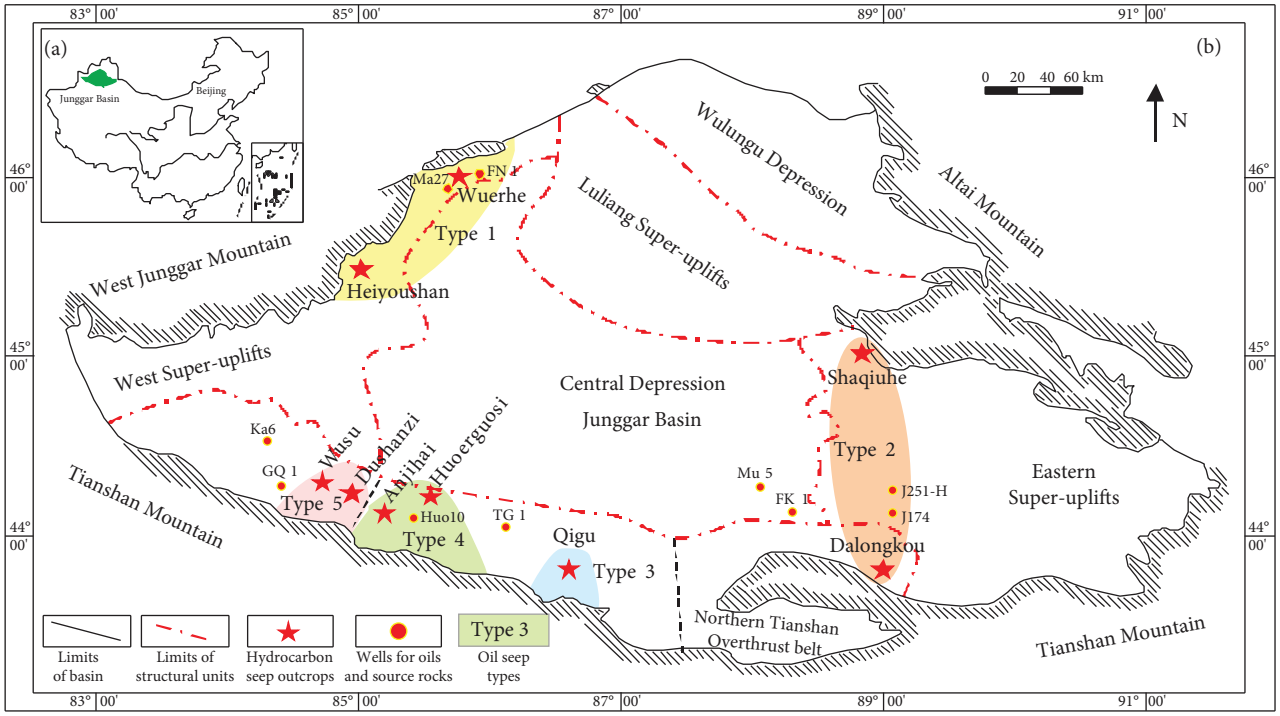

FIGURE 1: Location of the studied Junggar Basin in China (a) and the structural units and oil and gas seeps in the Junggar Basin, including the locations of the samples collected during this study (b).

spectrometer (MS) equipped with a Hewlett Packard 6890 II gas chromatograph. Gaseous components were separated in a gas chromatograph (GC), converted to CO_2 in a combustion interface, and then injected into the mass spectrometer. Individual hydrocarbon gas components (e.g., C_1–C_4) were separated using a fused silica capillary column (PLOT Q, 30 m × 0.32 mm). The GC oven used a heating ramp of 8°C/min from 35 to 80°C and 5°C/min up to 260°C, with this final temperature being maintained for 10 min. All gas samples were analyzed in triplicate, and the carbon isotopic values are reported in δ notation as per mil (‰) relative to the VPDB standard, relative to which the accuracy of measurements is estimated to be ±0.5‰.

4. Results

The EOM (Extracted Organic Matter) and SARA (Saturates, Aromatics, Resins, and Asphaltenes) data of twenty-three oil-seeps, six crude-oil, and eight source-rock samples are given in Table 1. The carbon isotopic compositions and index molecular geochemical parameters of these samples are given in Table 2.

TIC (total ion current); mass chromatograms at a *m*/*z* (mass/charge) of 177, 191, and 217; and plots of selected molecular geochemical parameters of the NW, SW, SM, SE, and E samples are shown in Figures 4–11.

5. Discussion

5.1. Genesis of Gas Seeps. The $\delta^{13}C_1$ (carbon isotope of methane) of the studied samples SW-3, SW-4, and SW-5 are −43.7‰, −43.2‰, and −42.4‰, respectively. The $\delta^{13}C_2$ (carbon isotope of ethane) of these samples are −26.3‰, −26.2‰, and −26.7‰, respectively. These values theoretically can be influenced by secondary alteration as the gas samples were collected from mud volcanos and thus were contacted with surficial water and atmosphere. In such conditions, carbon isotopes would change, e.g., extremely negative $\delta^{13}C_1$ values (less than −50.0‰) caused by microbial alteration [26]. However, the values of this study are consistent with those of the natural gases without secondary alteration reported in the study area [15]. As such, we believe that the data here can represent the original properties of gas and thus provide insights into the genesis of gas seeps [27, 28].

The three gas seeps in this study were derived from the thermal decomposition of OMs (organic matters) rather than from inorganic chemical reactions (e.g., Fischer–Tropsch), as these samples are characterized by $\delta^{13}C_1 < \delta^{13}C_2$ [27]. It has been widely believed that the $\delta^{13}C_2$ of gas represents the genesis of gas [28, 29]. In this study, the $\delta^{13}C_2$ of the three samples ranges from −26.7‰ to −26.2‰, indicative of humic-type gases ([30]; Figure 12). In the SW study area, the potential source rocks for generating gases include Permian and Jurassic strata [25, 31], but only the Jurassic swap coal-bearing source rocks have the $\delta^{13}C_2$ (−28‰ to −22‰; [32]) that are consistent with those of gas seeps in this study. Therefore, gas emitted from mud volcanoes in the Wusu and Dushanzi areas of this study is believed to be derived from Jurassic rocks.

$\delta^{13}C_1$ of the gases in this study, generally reflecting the maturity of gas, is lower than those Jurassic-sourced gases reported in previous studies (−40.7‰ to −32.6‰; Figure 12; [15, 33]). This indicates that the gases in this

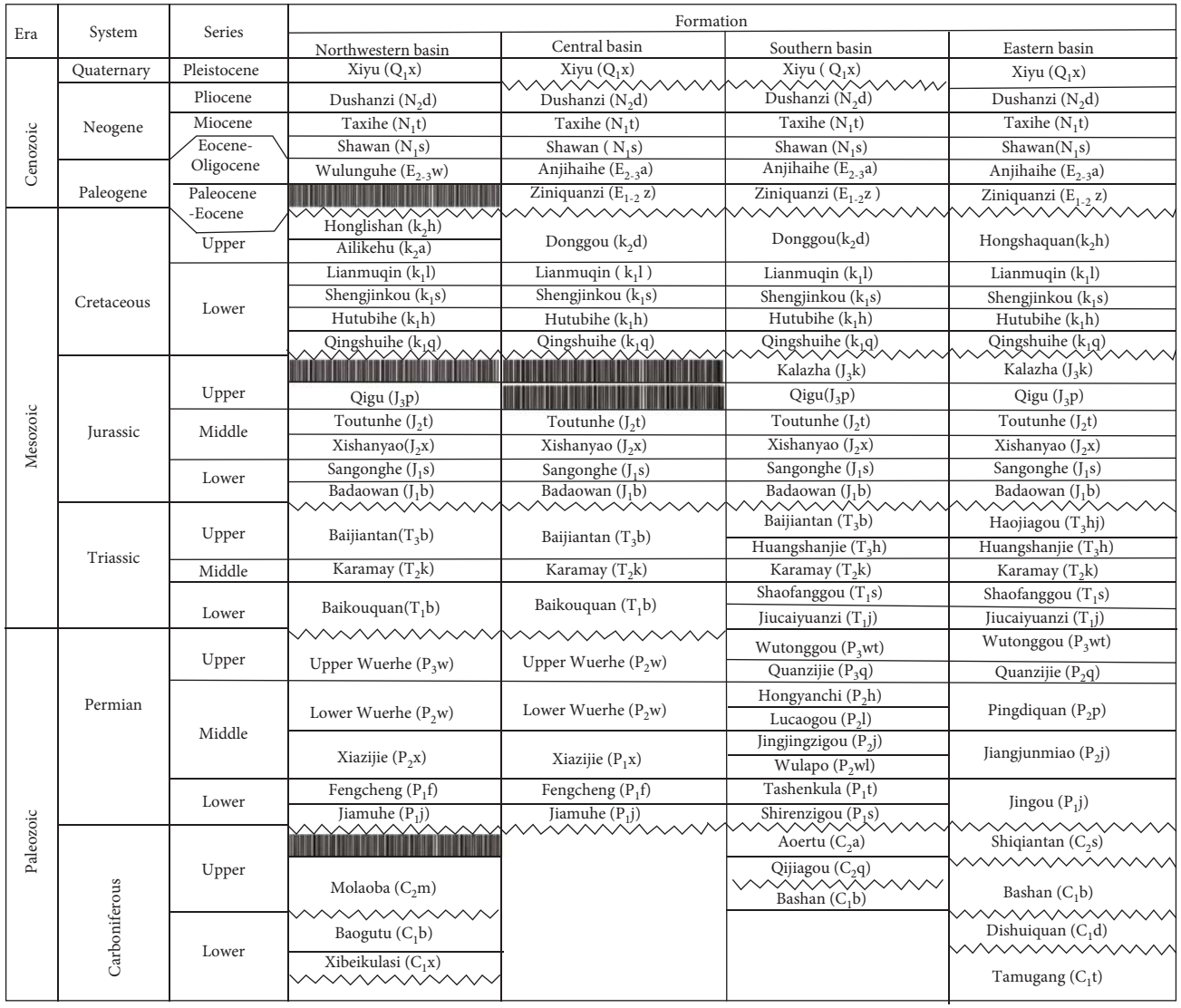

Figure 2: Generalized stratigraphic column in the Junggar Basin (after [76]). Note: the entire lower Cretaceous strata also called the Tugulu group (K_1tg; [8]).

study have relatively lower maturities, i.e., derived from the generation of Jurassic source rocks under low maturity (vitrinite reflectance < 0.6%; [34, 35]). This conclusion is consistent with the geological setting [25, 32]. In the southern Junggar Basin, the burial depth and associated thermal evolution of the Jurassic rocks in general show a gradually decrease from east to west. For example, rocks in the central segment of the southern Junggar are mature to highly mature [36]. In contrast, in the western segment of the southern Junggar, especially in the Dushanzi and Wusu areas of this study, the rocks are of low maturity to mature [33]. Therefore, the three gases of this study, located in the western segment of the southern Junggar Basin, are sourced from the generation of Jurassic rocks under low maturity.

In summary, we infer that the three gas seeps in the SW of the Junggar Basin are humic-type and were derived from Jurassic low-maturity source rocks.

5.2. Genesis of Oil Seeps

5.2.1. Oil Seeps in the Northwestern Basin (NW)

(1) General Properties of EOM and SARA Compositions. Six oil-seep samples were collected from Wuerhe and Heiyoushan outcrops in the NW (Figure 1(b)), including 2 bitumens, 2 oil sands, and 2 crude-oil seeps. The four solid oil seeps NW-1–NW-4 yield EOM content of 8.1% to 79.9% (Table 1), reflecting a large variation and oil origins. SARA analyses show that the four solid oil seeps NW-1–NW-4 are dominated by RA (SA/SARA = 0.11 – 0.16; Table 2). In contrast, the two crude-oil seeps NW-5–NW-6 are dominated by SA (SA/SARA = 0.80 – 0.82; Table 2). Theoretically, SARA fractions in oils generally follow the sequence of abundance SA>RA and the resistance to secondary alteration in the order of saturates<aromatics<resins<asphaltenes [37, 38]. In this study, samples NW-1–NW-4 have low values of SA/SARA, contrary to the typical sequence of

Table 1: Basic data of oil and gas seeps, selected crude oil, and source-rock samples from the Junggar Basin.

Number	Sample ID	Outcrops/depth (m)	Formation	Types of oil and gas seeps	EOM (%)	SARA fractions (%)			
						Saturates	Aromatics	Resins	Asphaltenes
1	NW-1	Wuerhe	K_1tg	Bitumen	8.10	7.60	2.80	35.70	44.50
2	NW-2	Wuerhe	K_1tg	Bitumen	79.90	9.60	5.10	38.40	36.90
3	NW-3	Wuerhe	K_1tg	Oil sand	37.80	7.70	4.40	37.90	40.00
4	NW-4	Heiyoushan	T_2k	Oil sand	15.30	8.30	3.70	37.50	42.00
5	NW-5	Heiyoushan	T_2k	Crude-oil seep	n.d.	61.70	11.80	15.40	1.10
6	NW-6	Heiyoushan	T_2k	Crude-oil seep	n.d.	60.00	12.40	16.10	1.80
7	Ma27	2347–2349	T_2k	Crude oil	n.d.	71.07	14.20	11.01	2.90
8	FN1	4254	P_1f	Source rock	0.40	57.49	16.07	25.45	0.91
9	FN1	4323	P_1f	Source rock	0.60	65.84	12.28	19.01	2.34
10	SW-1	Wusu	$E_{2-3}a$	Oil sand	1.30	82.40	12.50	4.10	1.00
11	SW-2	Wusu	$E_{2-3}a$	Oil sand	0.70	75.60	10.40	3.70	0.90
12	SW-3	Wusu	$E_{2-3}a$	Gas seep	n.d.	n.d.	n.d.	n.d.	n.d.
13	SW-4	Dushanzi	N_2d	Gas seep	n.d.	n.d.	n.d.	n.d.	n.d.
14	SW-5	Dushanzi	N_2d	Gas seep	n.d.	n.d.	n.d.	n.d.	n.d.
15	SW-6	Dushanzi	N_2d	Oil sand	0.10	n.d.	n.d.	n.d.	n.d.
16	Ka 6	3257–3260	$E_{2-3}a$	Crude oil	n.d.	65.36	13.71	8.36	6.50
17	GQ 1	4954–4956	$E_{2-3}a$	Crude oil	n.d.	77.35	11.02	8.98	2.54
18	GQ 1	5271	$E_{2-3}a$	Source rock	0.40	53.99	13.08	15.08	12.05
19	Ka 6	4253	J_2x	Source rock	0.50	61.83	14.62	12.95	1.53
20	SM-1	Anjihai	$E_{2-3}a$	Oil sand	0.10	n.d.	n.d.	n.d.	n.d.
21	SM-2	Anjihai	$E_{2-3}a$	Oil sand	0.20	n.d.	n.d.	n.d.	n.d.
22	SM-3	Anjihai	$E_{2-3}a$	Oil sand	0.10	n.d.	n.d.	n.d.	n.d.
23	SM-4	Huoerguosi	$E_{2-3}a$	Oil sand	0.20	73.40	16.00	8.80	1.20
24	SM-5	Huoerguosi	$E_{2-3}a$	Oil sand	0.40	71.40	14.10	13.80	0.50
25	SM-6	Huoerguosi	$E_{2-3}a$	Oil sand	1.90	71.50	13.00	6.50	2.50
26	SM-7	Huoerguosi	$E_{2-3}a$	Oil sand	0.90	66.20	17.60	14.60	0.80
27	SM-8	Huoerguosi	$E_{2-3}a$	Crude-oil seep	n.d.	81.90	7.90	8.20	1.50
28	SM-9	Qigu	J_3q	Crude-oil seep	n.d.	64.80	12.80	12.20	4.40
29	SM-10	Qigu	J_3q	Crude-oil seep	n.d.	68.80	16.00	12.20	2.20
30	SM-11	Qigu	J_3q	Crude-oil seep	n.d.	64.90	10.70	10.00	4.60
31	Huo 10	3159–3170	$E_{1-2}z$	Crude oil	n.d.	83.63	7.93	3.07	0.52
32	TG 1	3921	k_1tg	Source rock	0.60	61.38	9.48	22.66	1.51
33	SE-1	Dalongkou	P_2l	Bitumen	0.10	n.d.	n.d.	n.d.	n.d.
34	Mu 5	1300–1700	J_1s	Crude oil	n.d.	83.89	5.73	3.84	0.45
35	FK 1	3647	J_1s	Source rock	0.40	36.56	20.85	23.17	19.15
36	E-1	Shaqiuhe	J_1b	Oil sand	2.60	27.40	3.10	44.20	17.10
37	E-2	Shaqiuhe	J_1b	Oil sand	1.00	25.30	2.80	46.50	16.30
38	J251-H	4361–4976	P_2l	Crude oil	n.d.	52.18	14.41	19.35	4.12
39	J174	3135	P_2p	Source rock	2.48	60.53	16.32	19.55	2.67
40	J174	3314	P_2l	Source rock	0.40	43.92	19.29	29.64	6.53

EOM = Extracted Organic Matter, SARA = Saturates+Aromatics+Resins+Asphaltenes; n.d. = no data.

SA>RA. This indicates that these samples may have suffered from secondary alteration due to contact with surficial water and the atmosphere [26]. This also applies to the two crude-oil samples. However, the SARA compositions of the oils are normal as there are fresh oil charging later (see discussion in "(3) Molecular Geochemical Compositions" section for detail). As such, the original SARA compositions indicative of biodegradation were modified to normal.

(2) Carbon Isotopic Compositions. The carbon isotopic compositions ($\delta^{13}C_{VPDB}$) of the NW oil seeps are −28.9‰ to −27.5‰, which are slightly heavier than the Permian-

Figure 3: Photographs showing oil and gas seeps in the Junggar Basin. (a) The Shaqiuhe oil sand; (b) the Wuerhe bitumen; (c) the Heiyoushan crude-oil seep; (d) the Qigu crude-oil seep; (e) the Wusu mud volcano; (f) the Dushanzi mud volcano.

sourced crude oils and source rocks in the NW (−31.14‰ to −30.36‰; Table 2). Generally, with an increase of oil biodegradation, the oil $\delta^{13}C_{VPDB}$ would become heavier [26, 39]. As such, it can be implied that the NW oil seeps likely have suffered from secondary alteration as discussed above.

(3) Molecular Geochemical Compositions. Most of *n*-alkanes and isoprenoids (Pr and Ph) were removed, and the UCM (unresolved complex mixtures) hump is apparent in the TIC of the NW oil seeps (Figures 4(a) and 4(b); Table 2). These are all the typical evidences for secondary alteration (most likely biodegradation; [40]), consistent with the results and understanding above. All of the oil seeps studied here have *m*/*z* 177 mass chromatograms that indicate the presence of 25-norhopanes (Figures 4(d) and 4(e)), which is indicative of severe biodegradation [41, 42]. Therefore, we infer that the NW oil seeps in this study most likely have suffered from complex secondary alteration of petroleum in a process that may involve water washing, effusion of lighter composition hydrocarbons, and biodegradation [43, 44].

Interestingly, the crude-oil samples in the study area, although displaying TIC and *m*/*z* 177 mass chromatograms that contain UCM and 25-norhopanes indicative of severe biodegradation (Figures 4(c) and 4(f)), also detected some low- to middle-carbon-number *n*-alkanes, as evidenced by crude oil TIC mass chromatograms (Figures 4(a)–4(c)). The samples also display *m*/*z* 191 and 217 mass chromatograms that contain relatively complete terpane and sterane distribution (Figures 4(g)–4(l)). This suggests that early oil biodegradation was followed by one or more overprinting oil-charging events [45]. This may reflect the location of these samples within fault zones in the study area that may have focused fluid flow [46]. This is common in complex petroleum systems characterized by multiple stages of hydrocarbon migration, accumulation, and alteration [26].

(4) Source of Oil Seeps. Samples of oil seeps studied here, as discussed above, have suffered from severe secondary alteration, which may have modified the geochemical parameters and confuse interpretations regarding the genesis of oil seeps

Table 2: Molecular geochemical data of oil and gas seeps, selected crude oil, and source-rock samples from the Junggar Basin.

Number	Sample ID	1	2	3	4	5	6	7	8	9	10	11	12	13	14	15	16	17	18
1	NW-1	0.11	-28.10	n.d.	0.13	0.32	0.13	0.79	0.16	0.04	0.33	0.69	0.46	0.67	0.24	0.97	0.50	0.49	0.20
2	NW-2	0.16	-27.90	n.d.	0.14	0.86	0.76	0.81	0.27	0.04	0.34	0.65	0.49	0.66	0.30	0.97	0.51	0.49	0.25
3	NW-3	0.13	-27.80	n.d.	0.13	0.44	0.17	0.75	0.19	0.03	0.33	0.66	0.45	0.70	0.31	0.84	0.54	0.48	0.23
4	NW-4	0.13	-27.50	n.d.	0.13	0.68	0.59	0.61	0.17	0.04	0.32	0.79	0.48	0.61	0.29	0.95	0.56	0.58	0.21
5	NW-5	0.82	-28.90	n.d.	0.16	0.75	0.94	0.50	0.18	0.05	0.34	0.74	0.46	0.64	0.44	0.86	0.56	0.58	0.20
6	NW-6	0.8	-28.70	n.d.	0.15	0.93	0.97	0.67	0.21	0.05	0.36	0.70	0.45	0.57	0.37	0.89	0.56	0.58	0.23
7	Ma27	0.86	-30.36	1.29	0.18	0.95	0.88	0.45	0.15	0.02	0.24	0.56	0.44	0.86	0.17	0.70	0.42	0.41	0.18
8	FN1	0.74	-31.14	0.62	0.20	0.91	0.80	0.42	0.13	0.02	0.36	0.59	0.41	0.90	0.22	0.62	0.45	0.49	0.17
9	FN1	0.79	-30.68	0.72	0.18	0.98	0.65	0.31	0.10	0.03	0.25	0.46	0.42	0.99	0.21	0.62	0.46	0.48	0.16
10	SW-1	0.95	-28.60	1.30	0.76	1.34	0.81	1.83	0.11	0.98	0.15	0.64	0.38	0.49	1.11	0.41	0.49	0.49	0.41
11	SW-2	0.95	-28.40	1.20	0.92	0.76	0.58	1.95	0.08	0.86	0.16	0.73	0.31	0.47	1.20	0.35	0.58	0.53	0.39
15	SW-6	n.d.	-28.10	1.30	0.96	1.16	0.76	1.88	0.07	0.64	0.15	0.68	0.41	0.45	1.21	0.52	0.42	0.41	0.33
16	Ka6	0.84	-28.66	1.40	0.50	0.76	0.76	1.86	0.04	0.66	0.16	0.49	0.28	0.52	1.32	0.59	0.28	0.38	0.30
17	GQ1	0.88	-28.38	1.12	0.63	0.45	1.09	1.01	0.04	0.54	0.15	0.53	0.20	0.56	1.35	0.47	0.25	0.34	0.34
18	GQ1	0.71	-28.53	0.93	0.45	0.68	0.79	0.50	0.16	0.29	0.27	0.50	0.26	0.62	1.07	0.58	0.31	0.34	0.36
19	Ka6	0.84	-27.13	2.13	1.10	1.54	0.85	3.11	0.07	0.37	0.23	0.36	0.03	0.44	0.81	0.24	0.44	0.51	0.25
20	SM-1	n.d.	-30.40	0.70	0.82	0.55	0.94	0.72	0.06	1.09	0.11	0.51	0.66	0.53	1.17	0.49	0.46	0.48	0.37
21	SM-2	n.d.	-30.00	0.40	0.86	0.60	0.83	0.58	0.05	1.09	0.13	0.48	0.66	0.45	1.50	0.53	0.44	0.47	0.42
22	SM-3	n.d.	-29.60	0.60	0.90	0.64	0.94	0.82	0.05	1.34	0.10	0.54	0.76	0.50	1.24	0.42	0.49	0.49	0.44
23	SM-4	0.9	-29.90	0.50	0.72	0.63	0.88	0.62	0.04	1.31	0.10	0.49	0.71	0.54	1.19	0.50	0.49	0.50	0.42
24	SM-5	0.86	-29.90	0.50	0.87	0.58	0.92	0.58	0.06	1.50	0.12	0.57	0.74	0.54	1.33	0.46	0.50	0.52	0.46
25	SM-6	0.9	-30.30	0.90	0.90	0.64	0.93	0.51	0.07	1.44	0.11	0.54	0.65	0.49	1.24	0.61	0.46	0.48	0.48
26	SM-7	0.84	-29.30	0.60	0.74	0.74	0.93	0.50	0.05	1.49	0.11	0.56	0.66	0.51	1.17	0.62	0.48	0.50	0.42
27	SM-8	0.9	-28.80	0.60	0.95	0.56	0.91	0.50	0.05	1.64	0.09	0.48	0.71	0.41	1.28	0.61	0.51	0.53	0.42
28	SM-9	0.82	-28.00	1.80	1.16	0.95	1.11	1.87	0.06	0.68	0.19	0.30	0.12	0.26	0.53	0.55	0.56	0.54	0.32
29	SM-10	0.85	-27.80	2.40	1.12	0.97	1.07	1.86	0.06	0.67	0.18	0.33	0.12	0.37	0.56	0.54	0.54	0.52	0.26
30	SM-11	0.84	-28.30	1.80	1.07	0.91	1.05	1.76	0.06	0.69	0.19	0.31	0.13	0.26	0.51	0.60	0.56	0.53	0.28
31	Huo10	0.96	-30.75	0.80	0.55	0.55	0.97	0.59	0.04	1.24	0.14	0.53	0.50	0.62	1.41	0.32	0.44	0.48	0.40
32	TG1	0.75	-30.50	0.84	0.32	0.76	0.96	0.54	0.15	1.01	0.14	0.51	0.34	0.73	1.50	0.28	0.43	0.50	0.43
33	SE-1	n.d.	-29.40	1.00	0.22	0.84	0.96	0.84	0.05	0.21	0.20	0.61	0.25	0.41	0.37	0.80	0.35	0.39	0.18
34	Mu5	0.95	-27.39	3.82	1.04	0.87	1.15	2.43	0.03	0.45	0.23	0.40	0.06	0.42	0.83	0.42	0.41	0.54	0.37
35	FK1	0.78	-26.28	2.50	1.38	1.44	1.08	3.66	0.13	0.53	0.19	0.39	0.10	0.32	0.83	0.30	0.42	0.47	0.28
36	E-1	0.33	-29.80	n.d.	0.08	0.91	1.05	1.17	0.05	0.10	0.24	0.68	0.22	0.32	0.28	0.86	0.38	0.37	0.21
37	E-2	0.31	-29.20	n.d.	0.08	1.15	1.33	1.55	0.06	0.20	0.21	0.67	0.29	0.35	0.35	0.96	0.39	0.34	0.20
38	J251-H	0.74	-30.91	1.04	0.13	0.93	1.36	0.99	0.04	0.09	0.15	0.53	0.17	0.61	0.44	0.69	0.36	0.31	0.19
39	J174	0.78	-31.31	1.35	0.11	1.08	1.05	1.28	0.04	0.07	0.11	0.52	0.19	0.67	0.60	0.81	0.30	0.27	0.16
40	J174	0.64	-30.09	1.16	0.25	0.66	1.21	1.62	0.03	0.60	0.17	0.51	0.21	0.65	0.53	0.62	0.32	0.24	0.14

1: SA/SARA; 2: carbon isotopic composition of OM ($\delta^{13}C$ in ‰ relative to the VPDB standard); 3: pristane to phytane (Pr/Ph); 4: C_{19}/C_{20} tricyclic terpanes; 5: C_{20}/C_{21} tricyclic terpanes; 6: C_{21}/C_{23} tricyclic terpanes; 7: C_{24} tetra-/C_{26} tricyclic terpanes; 8: C_{24} tetracyclic terpane/C_{30} hopane; 9: Ts/Tm; 10: Tm/C_{30} hopane; 11: C_{29}/C_{30} hopanes; 12: gammacerane/C_{30} hopane; 13: C_{35}/C_{34}22S hopanes; 14: C_{27}/C_{28} $\alpha\alpha\alpha$20R regular steranes; 15: C_{28}/C_{29} $\alpha\alpha\alpha$20R regular steranes; 16: sterane $C_{29}\alpha\alpha\alpha$20S/(20R+20S); 17: sterane 20R$C_{29}\alpha\beta\beta/(\alpha\beta\beta+\alpha\alpha\alpha)$; 18: diasteranes/regular steranes. Note that where there is no indication of specific isomers, all isomers were used.

[26]. Meanwhile, the overprinting of the biodegradation information by the later charging of fresh oils makes it more difficult to determine the actual sources of these oil seeps [45]. However, combined with geological setting of source rocks, some biomarkers with relatively high resistance to biodegradation and fingerprints to unique organic facies may still provide some useful information to determine the sources of oil seeps [26].

The molecular geochemical components commonly used to analyze oil source could be generally divided into three types, including organic facies, OM inputs, and maturity. The parameters related to organic facies mainly contains β-carotanes associated with anoxic, hypersaline, or highly restricted lacustrine settings [26, 47], gammacerane representing evaporative or highly saline environments [26], the ratio of pristane to phytane (Pr/Ph) reflecting redox

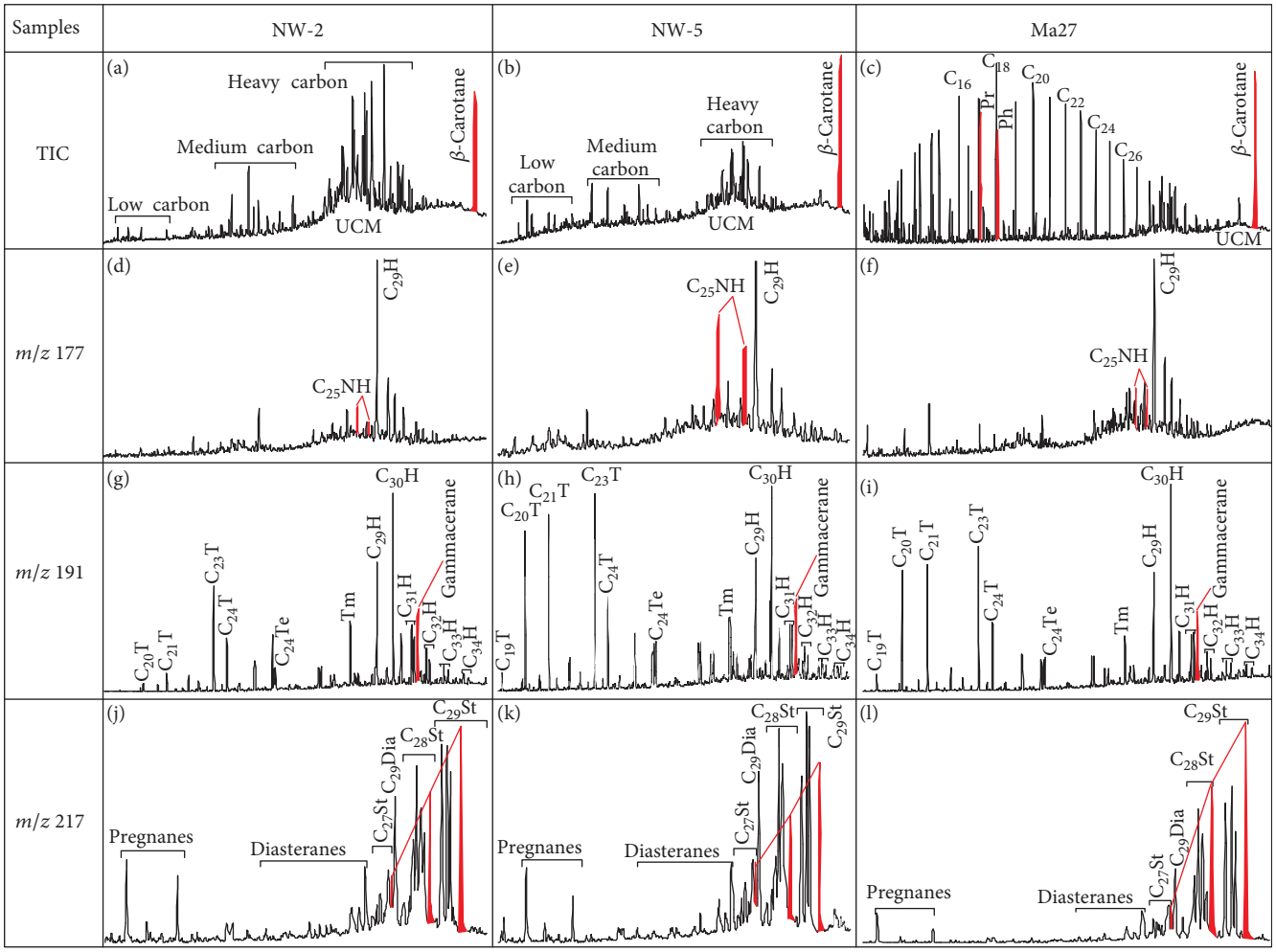

FIGURE 4: Selected molecular geochemical chromatograms of oil-seep and crude-oil samples from the northwestern Junggar Basin. TIC: total ion current mass chromatogram; UCM: unresolved complex mixture; T: tricyclic terpane; Te: tetracyclic terpane; NH: nor-hopane; H: hopane; Dia: diasteranes; St: steranes.

environments [48–50], and high ratios of $C_{29}H/C_{30}H$, $C_{35}/C_{34}22S$ close to anoxic conditions [26].

Terpane and sterane parameters can provide evidence of organic matter sources and the precursors of source rock [26, 45, 51, 52]. Lower C_{23} tricyclic terpane abundance relative to C_{19}, C_{20}, and C_{21} tricyclic terpanes and high C_{24} tetracyclic terpane abundance are indicative of the presence of significant amounts of terrigenous OM [53–55]. C_{27} steranes are believed to be derived predominantly from phytoplankton and metazoan sources, whereas C_{28} steranes are derived from specific types of phytoplankton (e.g., diatoms; [56]), and C_{29} steranes are derived from terrigenous higher plants [57, 58]. There are some exceptions to this in the form of pre-Devonian sediments and oils that developed during periods with no land-based higher plants [59, 60].

Parameters of maturity mainly include Ts/Tm [26] and sterane isomerization index $C_{29}\alpha\alpha\alpha S/(S+R)$ and $C_{29}\alpha\beta\beta/(\alpha\beta\beta+\alpha\alpha\alpha)$ [61, 62].

Most of the molecular geochemical parameters could be influenced in high biodegradation, so these parameters can also be used to reveal the process of biodegradation ([26]; see discussion in "(5) Secondary alteration (biodegradation) of oil seeps" section for detail). The resistance of biomarkers in organic matter to biodegradation generally follows the order *n*-alkanes<isoprenoid alkanes (Pr and Ph)<regular steranes<pentacyclic triterpane<Ts/Tm<gammacerane<tetracyclic terpanes<tricyclic terpanes<25-norhopane<diasteranes [26, 50]. Generally, with an increase in biodegradation of oils, the concentrations of *n*-alkanes and isoprenoid alkanes are reduced. In contrast, the *β*-carotanes, terpanes, and steranes are relatively unaffected by light or moderate secondary alteration and can still be used to study oil sources [26]. In this study, *n*-alkanes and isoprenoid alkanes have suffered degradation and may not be reliable indicators for constraining the genesis of the oil seeps. However, the distributions of terpanes and steranes are relatively undisturbed. Therefore, the relatively stable molecular compounds that we used to analyze the genesis of oil seeps are shown in Table 2 and Figure 5.

There are three sets of potential source rocks in the NW region, including lower Permian Jiamuhe (P_1j) and Fengcheng (P_1f) and middle Permian lower Wuerhe (P_2w) formations, and it has been widely believed that the Fengcheng Formation (P_1f) represents the main contributor

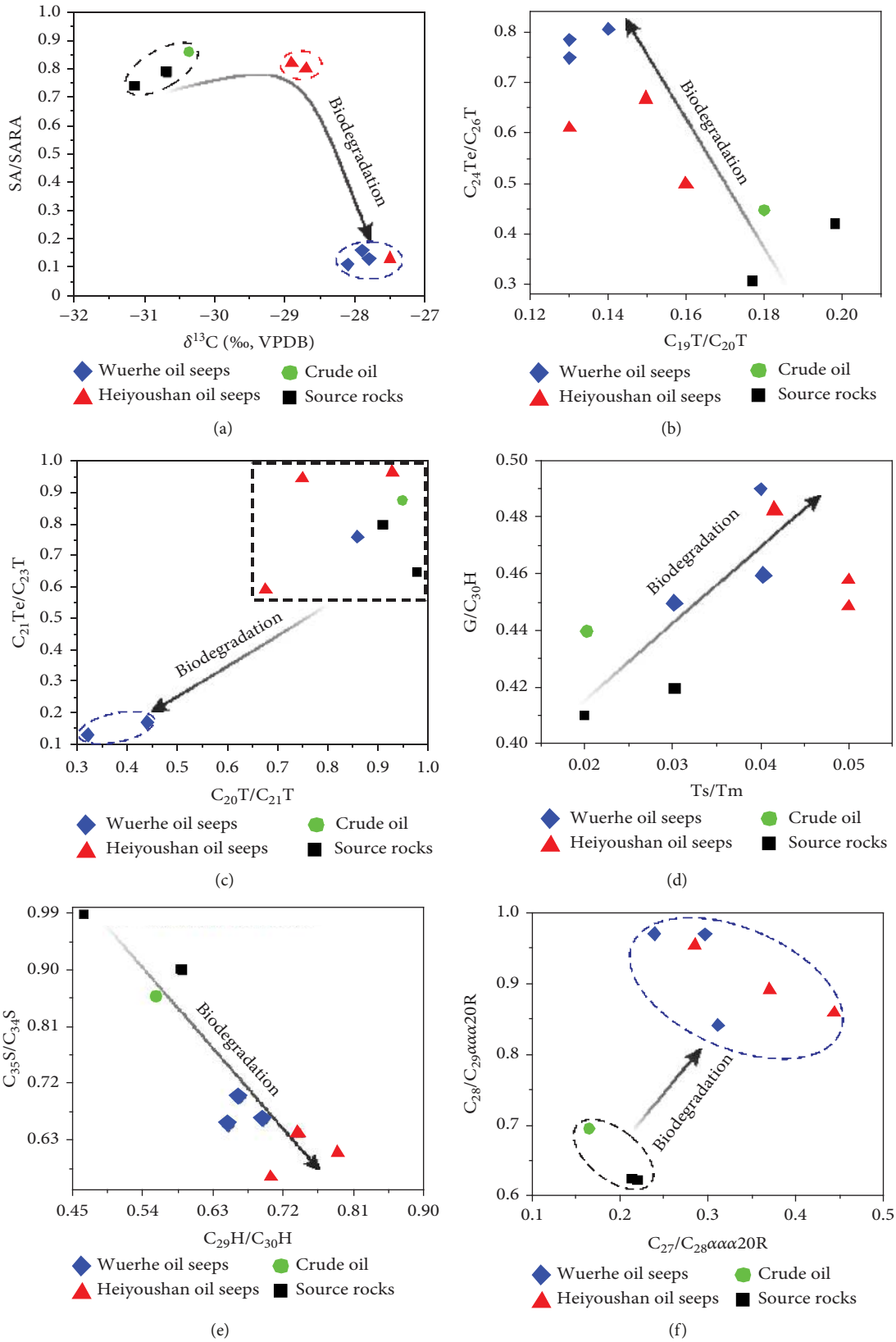

Figure 5: Continued.

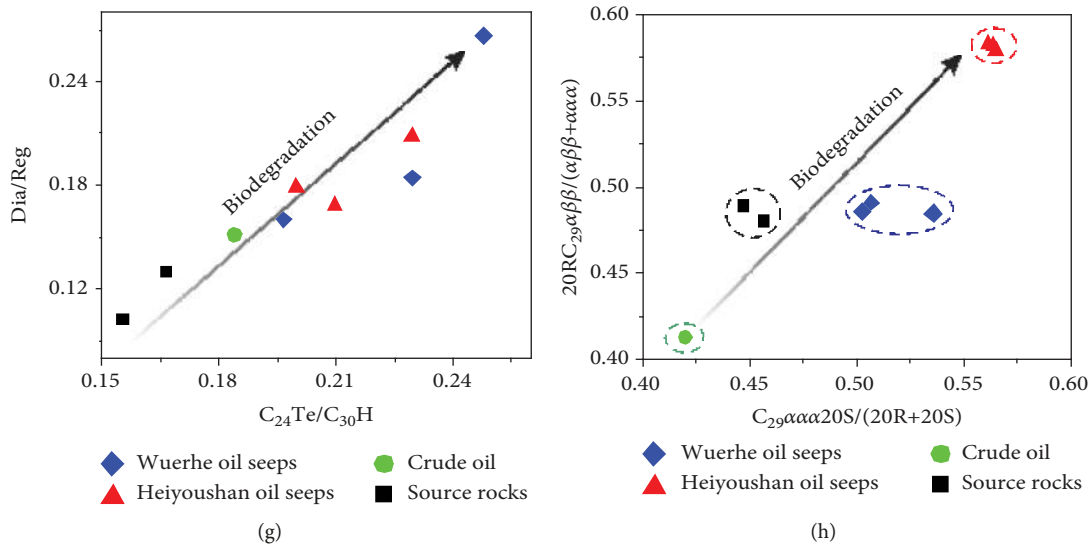

Figure 5: Plots of selected molecular geochemical parameters for oil-seep, crude-oil, and source-rock samples from the northwestern Junggar Basin. (a) $\delta^{13}C$ (in ‰ relative to the VPDB standard) vs. SA/SARA; (b) $C_{19}T/C_{20}T$ vs. $C_{24}Te/C_{26}T$; (c) $C_{20}T/C_{21}T$ vs. $C_{21}T/C_{23}T$; (d) Ts/Tm vs. $G/C_{30}H$; (e) $C_{29}H/C_{30}H$ vs. $C_{35}S/C_{34}S$; (f) C_{27}/C_{28} $\alpha\alpha\alpha$20R vs. C_{28}/C_{29} $\alpha\alpha\alpha$20R; (g) $C_{29}\alpha\alpha\alpha$20S/(20R+20S) vs. $C_{29}\alpha\beta\beta/(\alpha\beta\beta+\alpha\alpha\alpha)$; (h) $C_{24}Te/C_{30}H$ vs. Dia/Reg. Abbreviations: SA = saturates+aromatics in %; SARA = saturates+aromatics+resins+asphaltenes in %; T = tricyclic terpane; Te = tetracyclic terpane; G = gammacerane; H = hopane; S = 22S hopane; Dia = diasteranes; Reg = regular steranes. Data from Table 2.

of oil [8, 45]. Previous research indicates that the Fengcheng Formation (P_1f) contains elevated abundances of β-carotane and gammacerane and is the only source rock in the study area that was deposited in a highly saline lacustrine environment [47, 63]. This source rock is dominated by Type I kerogen and has high TOC values (1.26–4.92%) where this organic material was derived predominantly from algae [64]. The Fengcheng source rocks also have low Ts/Tm ratios (<0.1), low diasterane abundances, and tricyclic terpanes and regular steranes that increase in abundance in the order C_{20}–C_{21}–C_{23} and C_{27}–C_{28}–C_{29}, respectively [25]. All of these characteristics are consistent with the compositions of the samples analyzed in this study, indicating that the oil seeps in the study area were derived from the lower Permian Fengcheng Formation source rocks (Table 2; Figure 5).

The crude-oil and source-rock samples in the study area have molecular compositions similar to those of oil-seep samples discussed above (Figures 4 and 5; Table 2). These samples have very similar terpane and sterane parameters, especially those that reflect the source of organic material and the environment of deposition, such as the distribution of C_{20}–C_{21}–C_{23} tricyclic terpanes and C_{27}–C_{28}–C_{29} regular steranes, as well as the high β-carotane and gammacerane abundances present in these samples. However, there are also some minor differences in some of these parameters between crude-oil, source-rock, and oil-seep samples (Figure 5). They are indicative of biodegradation (see discussion in "(5) Secondary alteration (biodegradation) of oil seeps" section for detail).

In summary, the molecular evidences supporting the P_1f source rocks include high concentrations of β-carotane evident in TIC mass chromatograms (Figures 4(a) and 4(b)), low ratios of C_{19}/C_{20} tricyclic terpanes (0.13–0.16) (Figure 5(b); Table 2), the $C_{20}<C_{21}<C_{23}$ order of distribution of tricyclic terpanes (Figure 5(c); Table 2), low Ts/Tm values (0.04–0.05), high gammacerane index values (gammacerane/$C_{30}H$ = 0.45 – 0.49) (Figure 5(d); Table 2), and high values of C_{29}/C_{30} hopanes (0.65–0.79) and C_{35}/C_{34}22S hopanes (0.57–0.70) (Figure 5(e); Table 2) as evidenced in the *m/z* 191 mass chromatogram. These characteristics also include the $C_{27}<C_{28}<C_{28}$ distribution of $\alpha\alpha\alpha$20R regular steranes (Figure 5(f); Table 2) and low concentrations of diasteranes (Dia/Reg = 0.20 – 0.23) (Figure 5(g); Table 2) observed in the *m/z* 217 mass chromatogram. The sterane isomerization index ($C_{29}\alpha\alpha\alpha$S/(S+R) and $C_{29}\alpha\beta\beta/(\alpha\beta\beta+\alpha\alpha\alpha)$) values of these oil seeps are 0.50–0.56 and 0.48–0.58, respectively (Figure 5(h); Table 2), reflecting all samples are in mature with similar maturity [61, 62].

(5) Secondary Alteration (Biodegradation) of Oil Seeps. The oil seeps, even the crude oils studied here, have suffered from relatively severe secondary alteration (most likely biodegradation) as discussed above. The typical characteristics including UCM and 25-norhopanes were detected on the TIC and *m/z* 177 mass chromatograms (Figures 4(a)–4(f)), and their carbon isotopic compositions become heavier with the reducing of SA/SARA ratios (Figure 5(a)). However, it is difficult to determine the actual level of biodegradation using the standards established by Peters and Moldowan [61] due to the overprinting of the biodegradation information by the later charging of fresh oils ([45]; see discussion in "(3) Molecular geochemical compositions" section for detail). As the oil seeps share similar geochemical characteristics between crude-oil and source-rock samples (see discussion in "(4) Source of oil seeps" section for detail), some minor differences in some of the geochemical parameters between

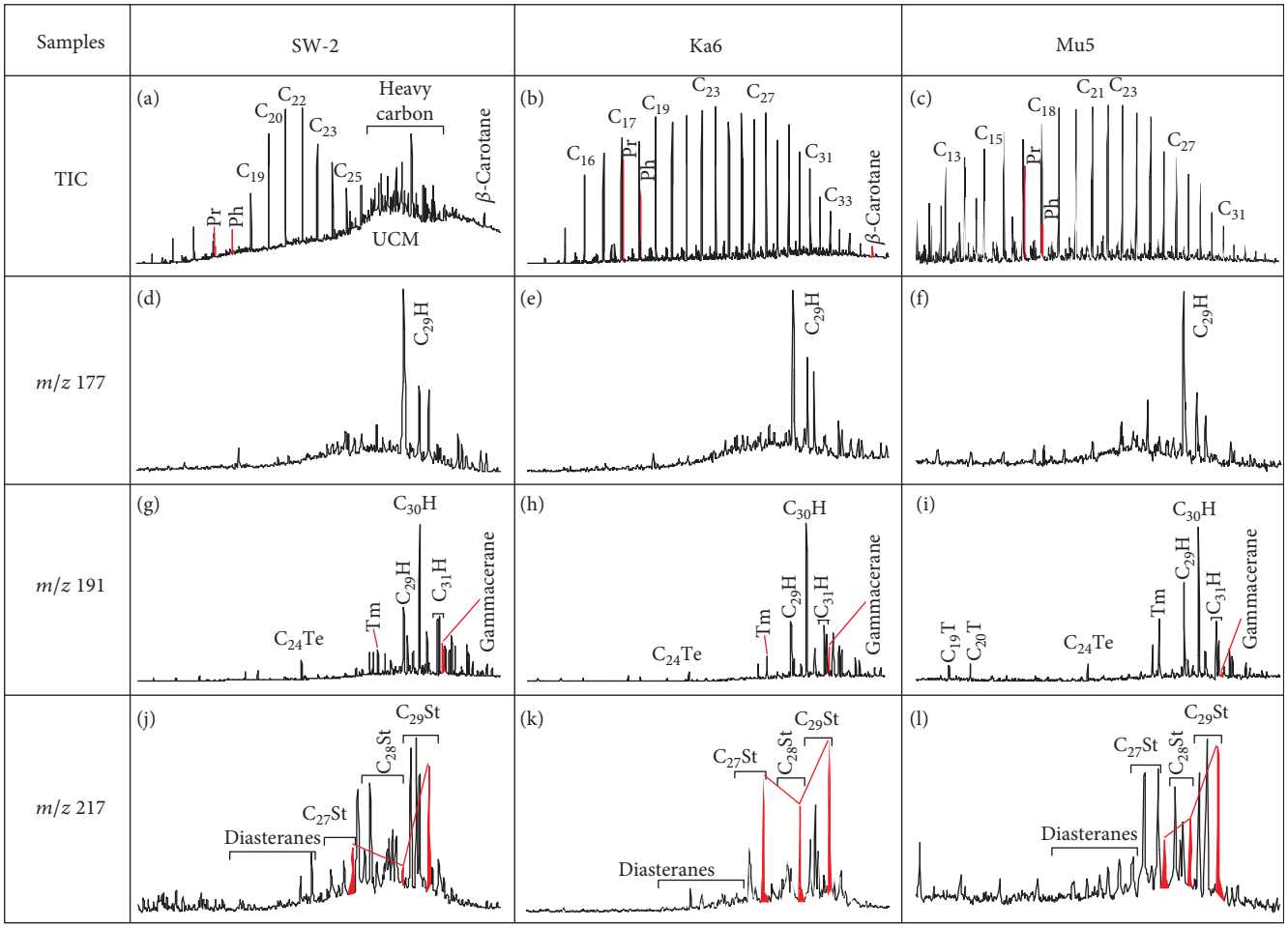

FIGURE 6: Selected molecular geochemical chromatograms of oil-seep and crude-oil samples from the western segment of southern Junggar Basin. See Figure 4 for the abbreviations.

crude-oil, source-rock, and oil-seep samples might provide insights into the process of secondary alteration (most likely biodegradation; [26]).

Tricyclic terpanes have a resistance to biodegradation in the order $C_{23}>C_{21}>C_{20}>C_{19}$ [42]. In this study, the values of C_{19}/C_{20}, C_{20}/C_{21}, and C_{21}/C_{23} tricyclic terpanes of samples decreased along the order of source rocks, crude oils, and oil seeps (Figures 5(b) and 5(c); Table 2). This implies the level of biodegradation. The resistance of some biomarkers to biodegradation in OM generally follows the order of regular steranes<hopanes ($C_{29}>C_{30}$)<Ts/Tm (Ts<Tm)<gammacerane<C_{26} tricyclic terpanes<C_{24} tetracyclic terpanes<diasteranes [26, 42, 50]. In this study, with the increasing of biodegradation, the ratios of C_{24} tetracyclic/C_{26} tricyclic terpane (Figure 5(b); Table 2), Ts/Tm, gammacerane/C_{30} hopane (Figure 5(d); Table 2), C_{29}/C_{30} hopanes (Figure 5(e); Table 2), C_{24} tetracyclic/C_{30} hopane, and diasteranes/regular steranes (Figure 5(g); Table 2) of samples increased, and the ratios of C_{35}/C_{34}22S hopanes of these samples decreased from source rocks to crude oils and to oil seeps (Figure 5(e); Table 2).

The isomerization steranes have a decreasing resistance to biodegradation in the order of $\alpha\alpha\alpha$20R>$\alpha\beta\beta$20R≥$\alpha\beta\beta$20S≥$\alpha\alpha\alpha$20S, and homologue steranes are resistant to biodegradation in the order of $C_{27}>C_{28}>C_{29}>C_{30}$ [62, 65]. In this study, the values of $C_{27}/C_{28}\alpha\alpha\alpha$20R, $C_{28}/C_{29}\alpha\alpha\alpha$20R (Figure 5(f); Table 2), $C_{29}\alpha\alpha\alpha$20S/(20R+20S), and 20R$C_{29}\alpha\beta\beta/(\alpha\beta\beta+\alpha\alpha\alpha)$ (Figure 5(h); Table 2) of samples increased from source rocks to crude oils and to oil seeps, indicative of biodegradation.

In summary, all the above results indicate that the oil seeps in the NW Junggar Basin were derived from the same source as that of the crude oils and OMs within source rocks encountered in wells close to oil seeps (Figure 1(b)), i.e., the lower Permian Fengcheng Formation. The oil seeps have undergone more severe biodegradation than crude oils and source rocks. Variable mixing amount of early secondary alteration of oil and later charging of fresh oil may result in phase variations, including crude oils, crude-oil seeps, solid oil sands, and bitumens [45].

5.2.2. Oil Seeps in the Western Segment of the Southern Basin (SW)

(1) General Properties of EOM and SARA Compositions. Three oil sand samples collected from Wusu and Dushanzi outcrops (Figure 1(b)) yield the EOM content of 0.1% to

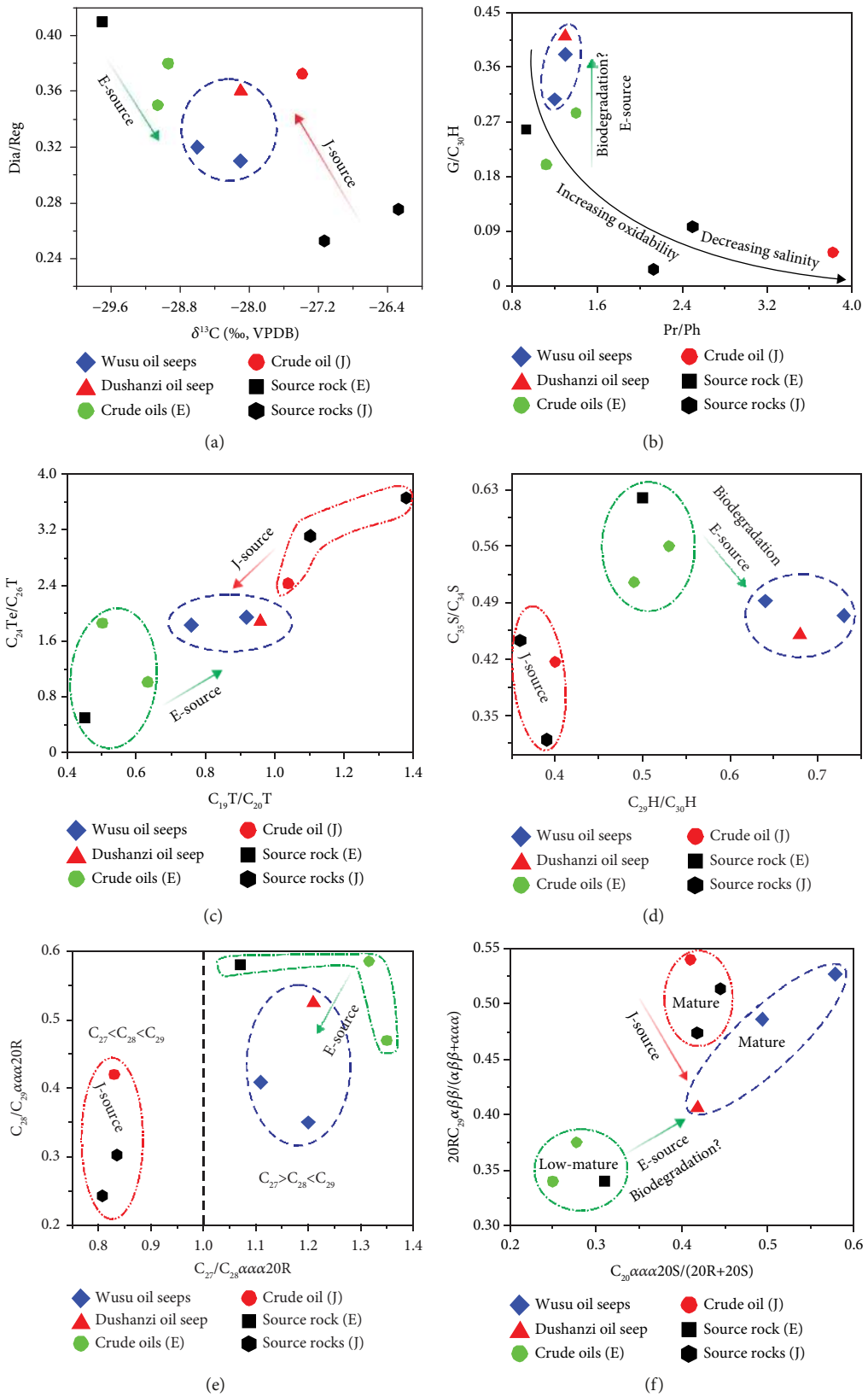

Figure 7: Plots of selected molecular geochemical parameters for oil-seep, crude-oil, and source-rock samples from the western segment of the southern Junggar Basin. (a) $\delta^{13}C$ (in ‰ relative to the VPDB standard) vs. Dia/Reg; (b) Pr/Ph vs. $G/C_{30}H$; (c) $C_{19}T/C_{20}T$ vs. $C_{24}Te/C_{26}T$; (d) $C_{29}H/C_{30}H$ vs. $C_{35}S/C_{34}S$; (e) C_{27}/C_{28} $\alpha\alpha\alpha$20R vs. C_{28}/C_{29} $\alpha\alpha\alpha$20R; (f) $C_{29}\alpha\alpha\alpha$20S/(20R+20S) vs. $C_{29}\alpha\beta\beta/(\alpha\beta\beta+\alpha\alpha\alpha)$. See Figure 5 for the abbreviations. Data from Table 2.

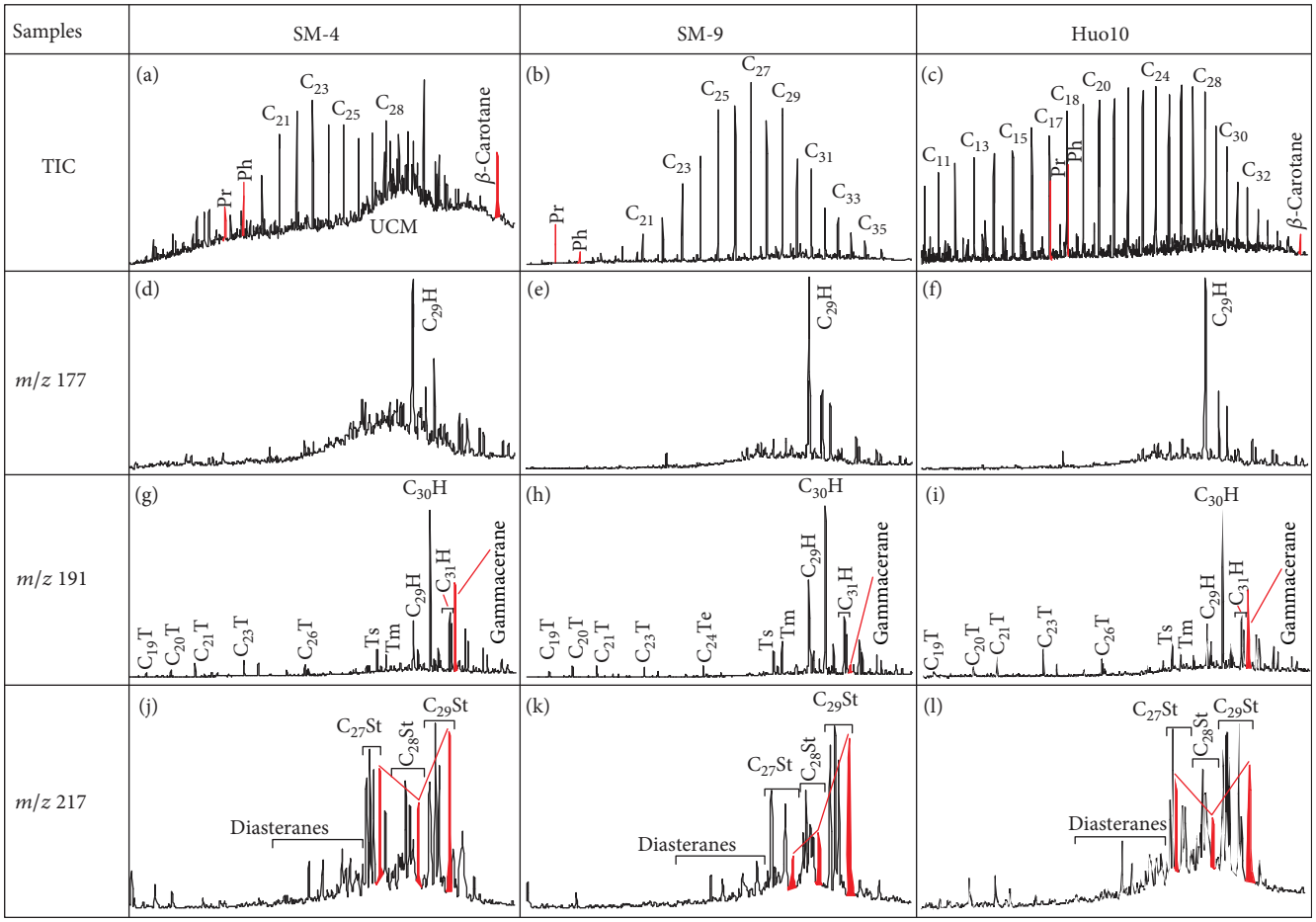

FIGURE 8: Selected molecular geochemical chromatograms of oil-seep and crude-oil samples from the middle segment of the southern Junggar Basin. See Figure 4 for the abbreviations.

0.7% (Table 1). SARA analyses show that they are dominated by SA (SA/SARA = 0.95) and have the typical sequence of SA>RA indicative of little secondary alteration (see discussion in "(1) General properties of EOM and SARA compositions" section for detail). Note that sample SW-6 has no SARA data due to low EOM content (0.1%) for analysis.

(2) Carbon Isotopic Compositions. The carbon isotopic compositions of oil sands in the SW region of the Junggar Basin are −29.6‰ to −28.1‰, which are slightly heavier than crude oils and source rocks from Paleogene (−28.66‰ to −28.38‰) but are lighter than Jurassic-derived oils and source rocks (−27.13‰ to −26.28‰) (Figure 7(a); Table 2). Therefore, we infer that the SW oil sands might be derived from Paleogene source rocks with secondary alteration (most likely biodegradation; see discussion in "(2) Carbon isotopic compositions" section for detail; [26, 39]) or mixing with Jurassic-derived oils. Given that the SARA compositions of the EOM are normal as discussed above ((1) General properties of EOM and SARA compositions section), the mixing interpretation is more likely.

(3) Molecular Geochemical Compositions. Oil sand samples studied here display TIC and *m*/*z* 177 mass chromatograms that contain apparent UCM hump without 25-norhopanes (Figures 6(a) and 6(d)), indicating that these samples have suffered from only slight secondary alteration (most likely biodegradation; see discussion in "(3) Molecular geochemical compositions" section). Interestingly, the UCM and 25-norhopanes were also not detected in TIC and *m*/*z* 177 mass chromatograms of the Paleogene- and Jurassic-derived crude oils in the southern basin, respectively (Figures 6(b), 6(c) and 6(e) and 6(f)). This is indicative of nonbiodegradation. Amount of low- to middle-carbon-number *n*-alkanes and isoprenoids (Pr and Ph) were detected, but most of the high-carbon-number *n*-alkanes that have more resistance to biodegradation were removed on TIC mass chromatograms (Figure 6(a)). The samples also display *m*/*z* 191 and 217 mass chromatograms that contain complete terpane and sterane distributions (Figures 6(g)–6(l)). All these suggests that oils were biodegraded only slightly, if present, and might have multistage oil charging events (see discussion in "(3) Molecular geochemical compositions" section for detail). This is different from the NW samples.

(4) Source of Oil Seeps. The oil sand samples studied here have only suffered from light biodegradation as discussed above. This may have not modified the geochemical parameters obviously [26]. However, the overprinting of later charging of fresh oils may complex the determination of actual

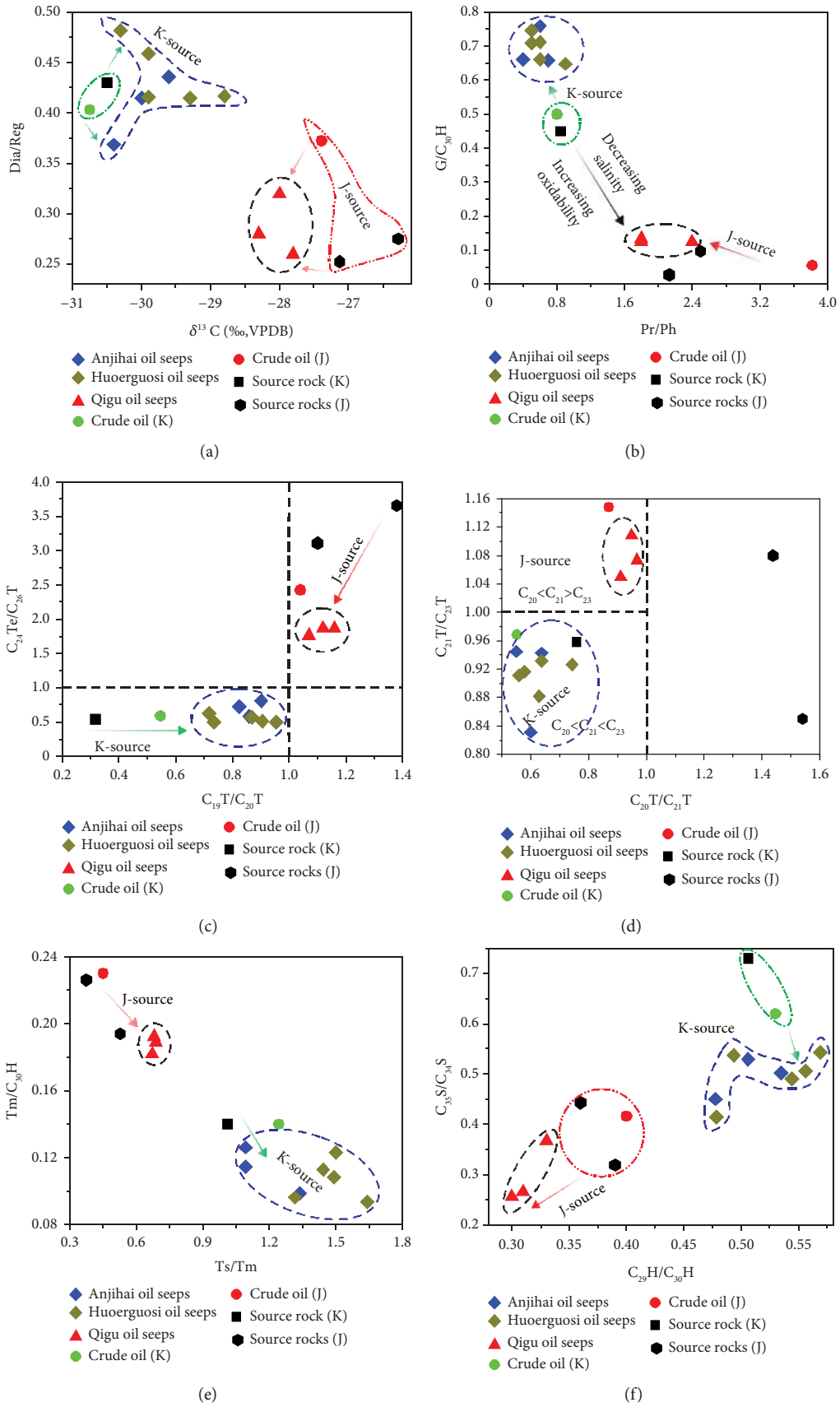

Figure 9: Continued.

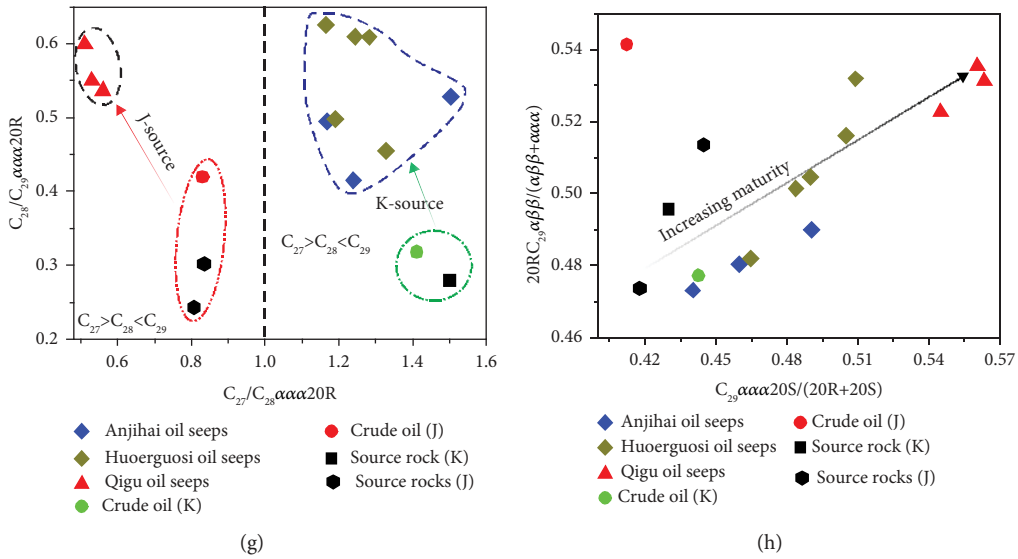

FIGURE 9: Plots of selected molecular geochemical parameters for oil-seep, crude-oil, and source-rock samples from the middle segment of the southern Junggar Basin. (a) $\delta^{13}C$ (in ‰ relative to the VPDB standard) vs. Dia/Reg; (b) Pr/Ph vs. G/C_{30}H; (c) $C_{19}T/C_{20}T$ vs. $C_{24}Te/C_{26}T$; (d) $C_{20}T/C_{21}T$ vs. $C_{21}T/C_{23}T$; (e) Ts/Tm vs. Tm/C_{30}H; (f) $C_{29}H/C_{30}H$ vs. $C_{35}S/C_{34}S$; (g) C_{27}/C_{28} $\alpha\alpha\alpha$20R vs. C_{28}/C_{29} $\alpha\alpha\alpha$20R; (h) $C_{29}\alpha\alpha\alpha$20S/(20R+20S) vs. $C_{29}\alpha\beta\beta/(\alpha\beta\beta+\alpha\alpha\alpha)$. See Figure 5 for the abbreviations. Data from Table 2.

source of oil sands [45]. Combined with geochemical characteristics of regional crude oils and source rocks in the SW, some molecular components with fingerprint to unique organic facies may also provide important data to determine the source of oil sands (see discussion in "(4) Source of oil seeps" section for detail; [26]).

The Paleogene lacustrine- and Jurassic swamp-facies strata have been widely believed to be the main source of oils within the SW [35, 66]. As shown in Table 2 and Figure 7, previous research indicates that the Jurassic-derived oils have heavy carbon isotopic compositions ($\delta^{13}C_{VPDB}$>−28‰), high values of Pr/Ph (>2.0), very low abundance of gammacerane with no β-carotane, and the regular steranes that increase in abundance in the order C_{27}-C_{28}-C_{29} [66], all of which indicate a low salinity and weakly oxidizing to oxidizing swamp facies [48–50, 67]. The Jurassic source rocks are dominated by Type II–III kerogens, of which OMs are mature–highly mature, indicating that they generated both oil and gas [66]. The Paleogene-derived oils differ from the Jurassic-derived oils in their lighter carbon isotopic compositions ($\delta^{13}C_{VPDB}$<−28‰), lower values of Pr/Ph (1.0–2.0), higher abundances of gammacerane and β-carotane, and the regular steranes C_{27}-C_{28}-C_{29} that define "V-shaped" distributions, all of which indicate a brackish to saline lacustrine facies [25, 68]. The Paleogene source rocks are dominated by Type I–II kerogens, of which OMs are low maturity–mature, indicating that they were involved in oil generation [66]. All of these characteristics contain the compositions of the samples analyzed in this study, indicating that the oil sands in the SW may be derived from the mixture of Jurassic- and Paleogene-source rocks (Figure 7; Table 2).

In detail, evidences supporting the mixture of Jurassic- and Paleogene-derived oils for the SW oil seeps include carbon isotopic compositions ($\delta^{13}C_{VPDB}$), the distributions of C_{19}, C_{20}, C_{21}, and C_{23} tricyclic terpanes and C_{24} tetracyclic terpanes, and sterane isomerization index ($C_{29}\alpha\alpha\alpha$S/(S+R) and $C_{29}\alpha\beta\beta/(\alpha\beta\beta+\alpha\alpha\alpha)$) (Figure 7; Table 2). The $\delta^{13}C_{VPDB}$ of the SW oil seeps fall in between Jurassic- (−27.13‰ to −26.28‰) and Paleogene-derived oils and source rocks (−28.66‰ to −28.38‰), which is consistent with the values of dia-/regular-steranes (Figure 7(a); Table 2). This suggests the source contribution from both Paleogene and Jurassic rocks (see discussion in "(4) Source of oil seeps" section for detail). The C_{19}–C_{23} tricyclic terpanes and C_{24} tetracyclic terpanes are indicative of kerogen types of OM (see discussion in "(4) Source of oil seeps" section for detail). Jurassic-derived oils and source rocks have higher values of C_{19}/C_{20}, C_{20}/C_{21}, and C_{21}/C_{23} tricyclic terpanes and C_{24} tetra-/C_{26} tricyclic terpanes than those of the Paleogene-derived oils and source rocks, indicating more terrigenous OM involved (Figure 7(c), Table 2; [53–55, 69–71]). Besides, analyses of sterane isomerization index ($C_{29}\alpha\alpha\alpha$S/(S+R) and $C_{29}\alpha\beta\beta/(\alpha\beta\beta+\alpha\alpha\alpha)$) indicate that the Jurassic-derived oils and source rocks have higher maturity (0.41–0.44 and 0.47–0.54) than Paleogene-derived oils and source rocks (0.25–0.31 and 0.34–0.38), which is consistent with the geological setting (i.e., deeper burial of Jurassic than Paleogene) (Figure 7(f); [66]). As apparently shown in Figures 7(a), 7(c), and 7(f), some of the geochemical parameters of oil seeps fall between Jurassic- and Paleogene-derived oils and source rocks. This further suggests that the SW oil seeps derived from the mixture of Jurassic and Paleogene source rocks.

Notably, geochemical parameters of the SW oil seeps, such as Pr/Ph, gammacerane/C_{30} hopane, C_{29}/C_{30} hopanes, C_{35}/C_{34}22S hopanes, and the distribution of regular steranes C_{27}-C_{28}-C_{29}, indicate that the oil seeps

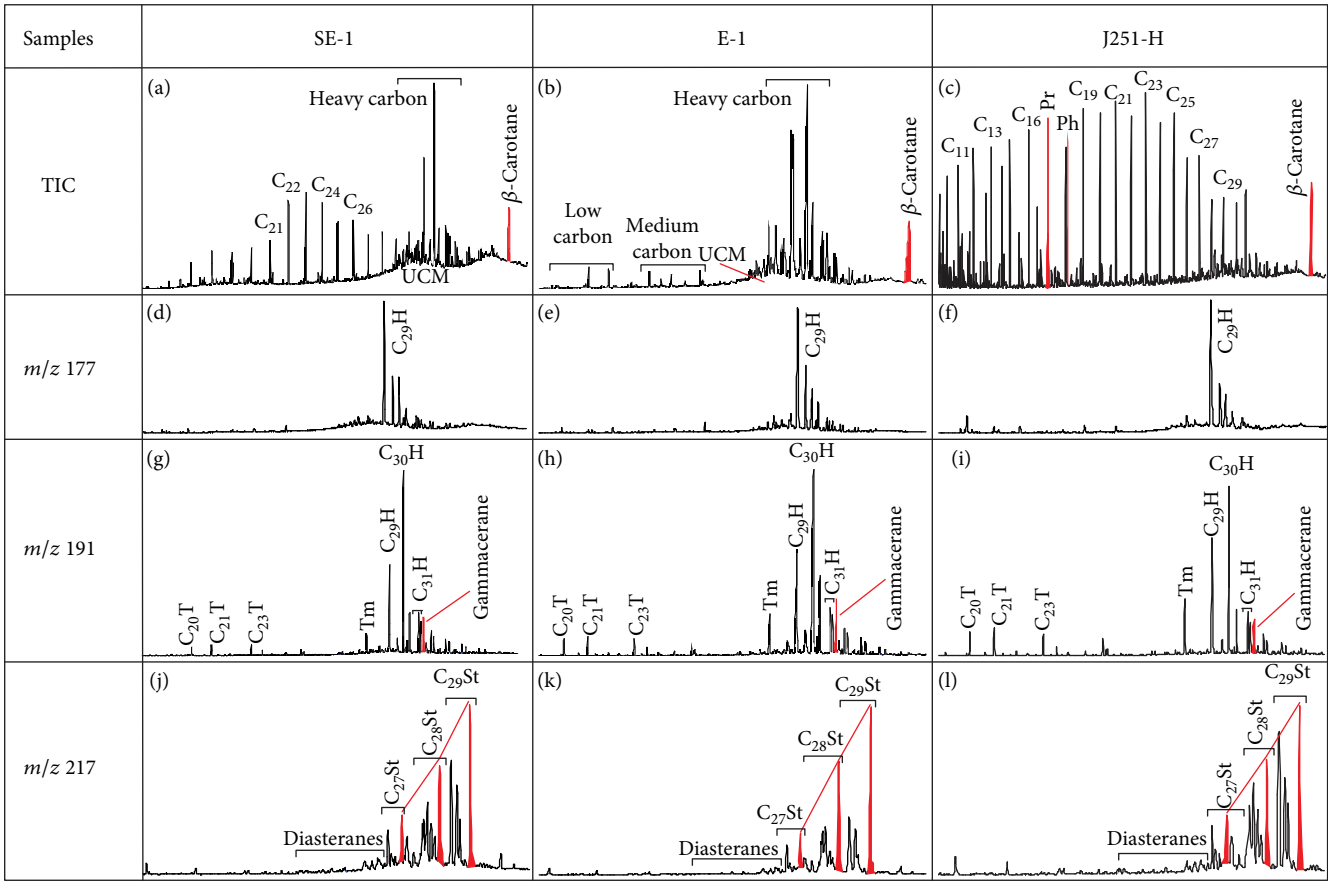

FIGURE 10: Selected molecular geochemical chromatograms of oil-seep and crude-oil samples from the eastern segment of the southern and eastern Junggar Basin. See Figure 4 for the abbreviations.

may be only derived from Paleogene source rocks. In detail, these samples have high values of gammacerane index (gammacerane/C_{30} hopane = 0.31 – 0.41) with low abundance of β-carotane and low ratios of Pr/Ph (1.2–1.3). These indicate a reducing and brackish environment for source rocks, consistent with the Paleogene source rocks (Figure 7(b); [25]). The geochemical parameters of C_{29}/C_{30} hopanes and C_{35}/C_{34}22S hopanes were related to depositional facies, of which weakly oxidizing coal-bearing swamp facies have lower ratios than reducing lacustrine facies [26]. As such, the oil seeps studied here were derived from Paleogene source rocks due to high values (Figure 7(d)). The distributions of regular steranes C_{27}-C_{28}-C_{29} could reflect the precursors of OM within source rocks (see discussion in "(4) Source of oil seeps" section for detail). The Jurassic-derived oils and source rocks are dominated by C_{29} steranes with increasing abundance in the order C_{27}-C_{28}-C_{29}, indicating the input of amount of terrigenous higher plants [57, 58]. However, the Paleogene-derived oils and source rocks have "V-shaped" distributions of regular steranes C_{27}-C_{28}-C_{29} with lower abundance of C_{28} steranes, suggestive of input of both terrigenous higher plants and phytoplankton [56]. In this study, the SW oil seeps were most likely derived from Paleogene rather than Jurassic source rocks (Figure 7(e)).

In summary, we infer that the isotopic and molecular geochemical compositions of the SW oil seeps have characteristics that are indicative of derivation from Paleogene source rocks as well as mixing with some Jurassic source rocks. Note that the actual mixing proportions of these two end members still need further studies to refine.

(5) Secondary Alteration (Biodegradation) of Oil Seeps. Samples of oil seeps in the SW have TIC mass chromatograms that indicate the presence of UCM. However, the high ratios of SA/SARA, complete distributions of low- and middle-carbon-number *n*-alkanes at TIC mass chromatograms, and the absence of 25-norhopanes at *m*/*z* 177 mass chromatograms all indicate that these samples might only suffer from a light biodegradation. The molecular geochemical parameters further confirm this conclusion (Figure 7). The parameters of the $\delta^{13}C_{VPDB}$, dia/regular steranes, C_{24} tetra-/C_{26} tricyclic terpanes, gammacerane/C_{30} hopane, and Tm/C_{30} hopane did not increase and C_{19}/C_{20} tricyclic terpanes did not decrease obviously from source rocks to crude oils and to oil seeps. This is different from that in the NW (see discussion in "(5) Secondary alteration (biodegradation) of oil seeps" section for detail). Therefore, the secondary alteration (most likely biodegradation) did not influence the main geochemical parameters and is not the major factor to the

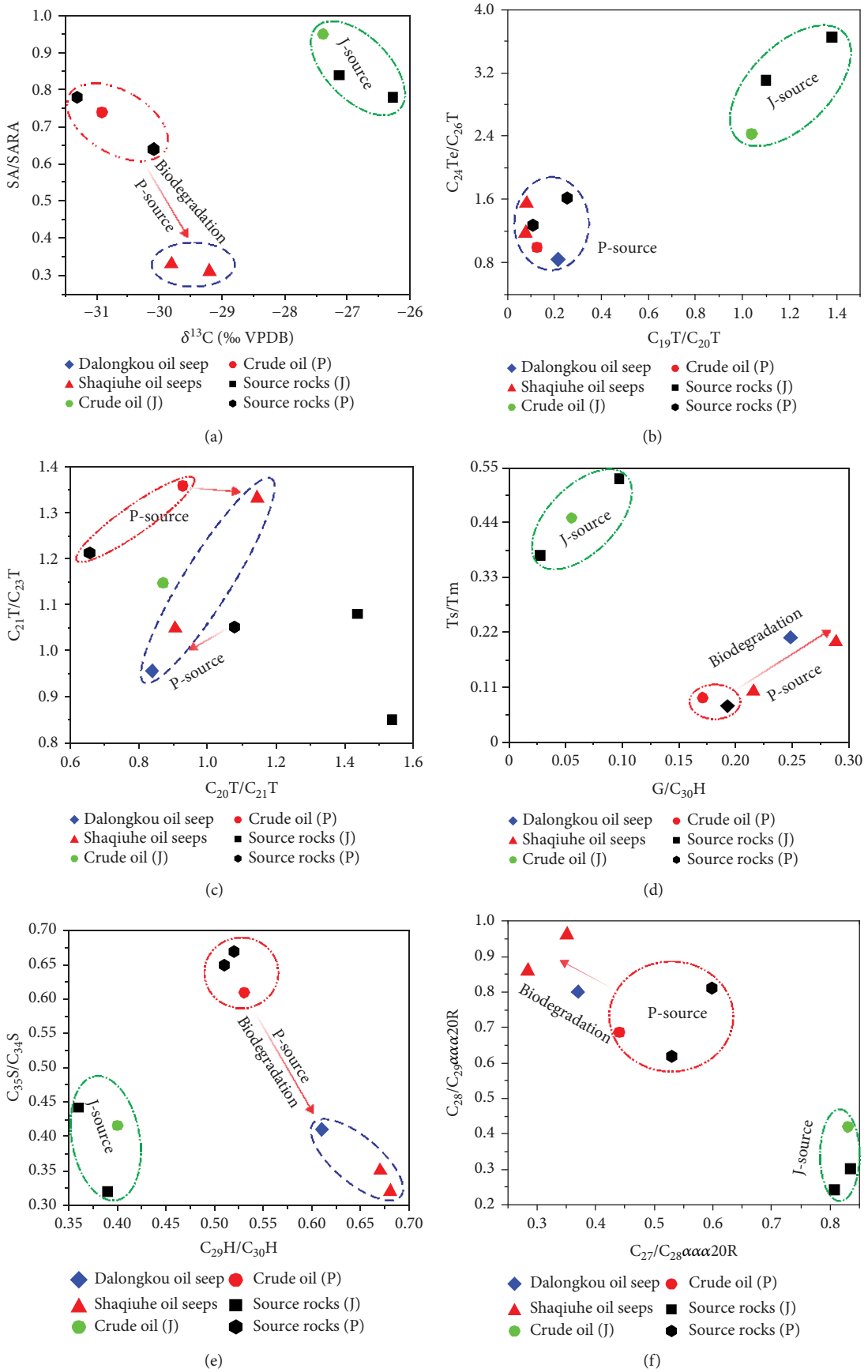

Figure 11: Continued.

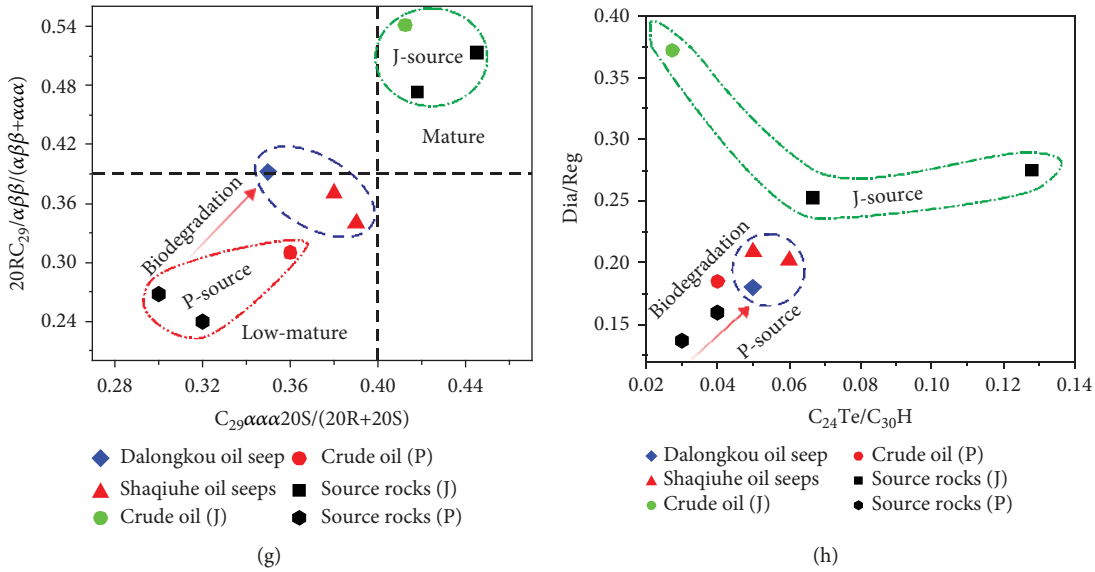

FIGURE 11: Plots of selected molecular geochemical parameters for oil-seep, crude-oil, and source-rock samples from the eastern segment of the southern and eastern Junggar Basin. (a) $\delta^{13}C$ (in ‰ relative to the VPDB standard) vs. SA/SARA; (b) $C_{19}T/C_{20}T$ vs. $C_{24}Te/C_{26}T$; (c) $C_{20}T/C_{21}T$ vs. $C_{21}T/C_{23}T$; (d) $G/C_{30}H$ vs. Ts/Tm; (e) $C_{29}H/C_{30}H$ vs. $C_{35}S/C_{34}S$; (f) C_{27}/C_{28} $\alpha\alpha\alpha$20R vs. C_{28}/C_{29} $\alpha\alpha\alpha$20R; (g) $C_{29}\alpha\alpha\alpha$20S/(20R+20S) vs. $C_{29}\alpha\beta\beta/(\alpha\beta\beta+\alpha\alpha\alpha)$; (h) $C_{24}Te/C_{30}H$ vs. Dia/Reg. See Figure 5 for the abbreviations. Data from Table 2.

formation of oil seeps in the study area. We speculate that the minor differences in some of the geochemical parameters between crude oils, source rocks, and oil seeps might be ascribed to complex mixture process between Paleogene- and Jurassic-derived oils with different maturities.

5.2.3. Oil Seeps in the Middle Segment of the Southern Basin (SM)

(1) General Properties of EOM and SARA Compositions. Eleven oil seep samples SM-1–11, which were collected from Anjihai, Huoerguosi, and Qigu outcrops in the middle segment of the southern basin (SM; Figure 1(b)), yield EOM content of 0.1% to 1.9% (Table 1). SARA analyses indicate that they are dominated by SA (SA/SARA = 0.82 – 0.90) except for the SM-1–SM-3 samples that have low EOM contents and thus are unsuitable for SARA analyses, implying that these samples may have not suffered from secondary alteration (see discussion in "(1) General properties of EOM and SARA compositions" section for detail).

(2) Carbon Isotopic Compositions. Carbon isotopic compositions ($\delta^{13}C_{VPDB}$) of the SM oil seeps range from −30.4‰ to −27.8‰, which vary in different outcrops (Table 2). In detail, the samples collected from Anjihai and Huoerguosi areas have relatively lighter $\delta^{13}C_{VPDB}$ (−30.4‰ to −28.8‰), which are similar with Cretaceous-derived oils and source rocks (−30.75‰ to −30.5‰). However, the oil-seep samples within the Qigu outcrop have relatively heavier $\delta^{13}C_{VPDB}$ (−28.3‰ to −27.8‰), which is similar with the Jurassic-derived oils and source rocks (Table 2). As such, we infer that the oil seeps from Anjihai and Huoerguosi outcrops may be derived from Cretaceous source rocks, while the Qigu oil seeps may be derived from Jurassic source rocks.

(3) Molecular Geochemical Compositions. The possible different oil sources for the SM seeps as discussed above were further constrained by their molecular geochemical compositions. Results from Anjihai and Huoerguosi outcrops indicated that UCM hump is apparent in the TIC but 25-norhopanes are absent in *m/z* 177 mass chromatograms (Figures 8(a) and 8(d)). This implies that these samples have suffered from secondary alteration (most likely biodegradation) but not severe (see discussion in "(3) Molecular geochemical compositions" section for detail). Amount of low- to middle-carbon-number *n*-alkanes and isoprenoids (Pr and Ph) were detected, but most of high-carbon-number *n*-alkanes that have more resistance to biodegradation were removed in TIC mass chromatograms (Figure 8(a)). In addition, the samples also display *m/z* 191 and 217 mass chromatograms that contain complete terpane and sterane distributions (Figures 8(g) and 8(j)). These suggest that early lightly biodegraded oils might be followed by one or more overprinting oil-charging events, similar to the SW oil seeps above (see discussion in "(3) Molecular geochemical compositions" section for detail).

However, UCM and 25-norhopanes are absent in the TIC and *m/z* 177 mass chromatograms of the Qigu samples (Figures 8(b), 8(c), 8(e) and 8(f)), indicating that no secondary alteration has occurred. Therefore, these samples have complete distributions of *n*-alkanes, terpanes, and steranes in TIC, *m/z* 191, and *m/z* 217 mass chromatograms, respectively (Figures 8(b), 8(c), 8(h), 8(i), 8(k) and 8(l)).

As discussed above, in the SM oil seeps, only the samples collected from Anjihai and Huoerguosi outcrops have suffered secondary alteration (most likely biodegradation). The biodegradation is only slight, and thus, such biodegradation

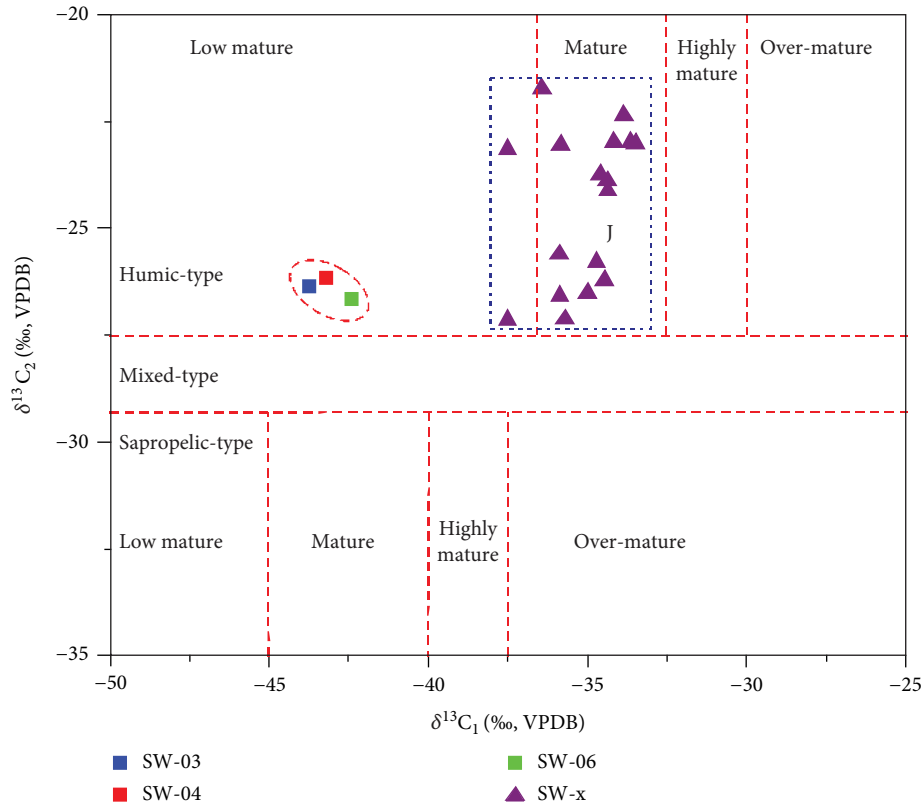

FIGURE 12: Plots of $\delta^{13}C_2$ (ethane) vs. $\delta^{13}C_1$ (methane) for gas seeps in the Junggar Basin. Note: the dataset SW-x is from Sun et al. [77] and represents subsurface reservoir samples. The boundary lines for different genetic and maturation groups are modified after Dai [78] and Tao et al. [34]. Please see Tao et al. [34] for the discussion and definition of the boundaries for detail.

did not influence the main geochemical parameters and is not the major factor to determinate the source of oil seeps in the study area.

(4) Source of Oil Seeps. The SM oil seeps in this study, as discussed above, have been limitedly influenced by secondary alteration, indicating that molecular geochemical parameters of the seeps may have not be modified obviously and thus can be used in oil-source analysis [26]. The overprinting of later charging of fresh oils may also do not disturb the determination of oil source of the seeps (see discussion in "(4) Source of oil seeps" section for detail). As such, combined with molecular geochemical composition of the oils and source rocks in the study area, some geochemical parameters with high fingerprint to organic facies may provide vital information to determine the source of oil seeps (Table 2; Figure 9; [26]).

There are two sets of potential source rocks in the SM, including Cretaceous lacustrine and Jurassic swamp-facies source rocks [31, 66]. The Cretaceous and Jurassic source rocks are mature–highly mature and are dominated by Type I–II and Type II–III kerogens, respectively, indicating that they were involved in oil generation [66]. Index geochemical characteristics of Jurassic-derived oils and source rocks in the study area have been discussed detailed above (see "(4) Source of oil seeps" section). Different from the Jurassic-derived oils and source rocks, the Cretaceous-derived oils and source rocks have relatively lighter carbon isotopic compositions ($\delta^{13}C_{VPDB}$<−29‰), low values of Pr/Ph (<1.0), high abundances of β-carotane and gammacerane (gammacerane/C_{30} hopane > 0.3), and regular steranes C_{27}-C_{28}-C_{29} that define "V-shaped" distributions, indicating a reducing saline lacustrine facies [25, 26, 50]. Notably, geochemical characteristics of Cretaceous-derived oils and source rocks are somewhat similar to those of Paleogene age, but the former have relatively lighter $\delta^{13}C_{VPDB}$, lower values of Pr/P, and higher abundances of β-carotane and gammacerane (see "(4) Source of oil seeps" section).

Based on these distinguishing standards, the oil seeps in Anjihai and Huoerguosi outcrops are deduced to be derived from Cretaceous source rocks, while in the Qigu seeps were most likely to be derived from Jurassic source rocks (Figure 9; Table 2). In detail, molecular geochemical compositions indicative of Cretaceous source rocks include light $\delta^{13}C_{VPDB}$ values (−30.4‰ to −28.8‰; Figure 9(a); Table 2), low Pr/Ph values (0.4–0.9; Figure 9(b); Table 2), high concentrations of β-carotane evident in TIC mass chromatograms (Figures 8(a)–8(c)), low values of C_{19}/C_{20} tricyclic terpanes (0.72–0.95) and C_{24} tetra-/C_{26} tricyclic terpanes (0.50–0.82; Figure 9(c); Table 2), C_{20}<C_{21}<C_{23} order of distribution of tricyclic terpanes (Figure 9(d); Table 2), high Ts/Tm (1.09–1.64) and low Tm/C_{30} hopane (0.09–0.13; Figure 9(e); Table 2) values, high gammacerane index

values (gammacerane/C_{30}H = 0.65 – 0.76) (Figure 9(b); Table 2), and high C_{29}/C_{30} hopanes (0.48–0.57) and C_{35}/C_{34}22S hopane (0.41–0.54) (Figure 9(f); Table 2) values as evidenced in the *m*/*z* 191 mass chromatogram. These characteristics also include the "V-shaped" distributions of C_{27}-C_{28}-C_{29} *ααα*20R regular steranes (Figure 9(g); Table 2) and relatively high concentrations of diasteranes (Dia/Reg = 0.37 – 0.48) (Figure 9(a); Table 2) observed at the *m*/*z* 217 mass chromatogram. The sterane isomerization index (C_{29}*ααα*S/(S+R) and C_{29}*αββ*/(*αββ*+*ααα*)) values of these oil seeps are 0.44–0.51 and 0.47–0.53, respectively (Figure 9(h); Table 2), reflecting all samples are mature with similar maturities [61, 62].

In contrast, the molecular geochemical compositions of the Qigu oil seeps have characteristics that are indicative of derivation from the Jurassic source rocks. These characteristics mainly include heavy $\delta^{13}C_{VPDB}$ values (−28.3‰ to −27.8‰; Figure 9(a); Table 2), high Pr/Ph values (1.8–2.4; Figure 9(b); Table 2), high values of C_{19}/C_{20} tricyclic terpanes (1.07–1.16) and C_{24} tetra-/C_{26} tricyclic terpanes (1.76–1.87; Figure 9(c); Table 2), low Ts/Tm (0.67–0.69), high Tm/C_{30} hopane (0.18–0.19; Figure 9(e); Table 2) values, low gammacerane index values (gammacerane/C_{30}H = 0.12 – 0.13; Figure 9(b); Table 2), and low values of C_{29}/C_{30} hopanes (0.30–0.33) and C_{35}/C_{34}22S hopanes (0.26–0.37) (Figure 9(f); Table 2) as evidenced in the *m*/*z* 191 mass chromatogram. These characteristics also include the regular steranes that increase in abundance in the order C_{27}-C_{28}-C_{29} (Figure 9(g); Table 2) and low concentrations of diasteranes (Dia/Reg = 0.26 – 0.32; Figure 9(a); Table 2) observed in the *m*/*z* 217 mass chromatogram. The sterane isomerization index (C_{29}*ααα*S/(S+R) and C_{29}*αββ*/(*αββ*+*ααα*)) values of these oil seeps are 0.54–0.56 and 0.52–0.54, respectively (Figure 9(h); Table 2), indicating that all samples are mature–highly mature with similar maturities [61, 62].

In summary, based on the above results and discussion, we infer that the oil seeps from Anjihai and Huoerguosi outcrops were derived from Cretaceous source rocks and the oil seeps from Qigu outcrop were sourced from Jurassic rocks.

5.2.4. Oil Seeps in the Eastern Segment of the Southern (SE) and Eastern (E) Basin

(1) General Properties of EOM and SARA Compositions. Three oil-seep samples, which were collected from Dalongkou outcrop in the SE and Shaqiuhe outcrop in the E (Figure 1(b)), yield EOM content of 0.1% to 2.6% (Table 1). SARA analyses indicate that they are dominated by RA (SA/SARA = 0.31 – 0.33; Table 2), which do not show the typical sequence of SA>RA of normal oils. This implies that these samples have suffered from secondary alteration (see discussion in "(1) General properties of EOM and SARA compositions" section for detail). Note that sample SE-1 does not have SARA data due to low EOM content (0.1%).

(2) Carbon Isotopic Compositions. Carbon isotopic compositions ($\delta^{13}C_{VPDB}$) of oil seeps in the SE and E range from −29.8‰ to −29.2‰. These values, compared with the two possible source rocks in the study area, are slightly heavier than the Permian-derived oils and source rocks and greatly lighter than the Jurassic-derived oils and source rocks (Table 2). Considering that the $\delta^{13}C_{VPDB}$ of OM may become heavier with an increase in secondary alteration [26, 39], we infer that the oil seeps in the SE and E were most likely derived from Permian source rocks and subjected to certain secondary alteration (see discussion in "(3) Molecular geochemical compositions" section for detail).

(3) Molecular Geochemical Compositions. Analyses of molecular geochemical compositions of oil seeps studied here show that UCM hump is apparent in the TIC mass chromatograms but the 25-norhopanes are absent in the *m*/*z* 177 mass chromatograms (Figures 10(a), 10(b), 10(d) and 10(e)). This suggests that these samples have been subjected to slight secondary alteration (most likely biodegradation; see discussion in "(3) Molecular geochemical compositions" section for detail). Some of the low- to middle-carbon-number *n*-alkanes and isoprenoids (Pr and Ph) were detected on the TIC (Figures 10(a) and 10(b)). These samples also display *m*/*z* 191 and 217 mass chromatograms that contain relatively complete terpane and sterane distributions (Figures 10(g), 10(h), 10(j) and 10(k)). All these suggest that early lightly biodegraded oils were followed by one or more overprinting oil-charging events later (see discussion in "(3) Molecular geochemical compositions" section for detail).

Samples of oil seeps in the SE and E have only suffered from lightly secondary alteration as discussed above, which could not influence the main geochemical parameters and is not the major factor to determinate the source of oil seeps in the study area (see discussion in "(3) Molecular geochemical compositions" section for detail). In contrast, UCM and 25-norhopanes were not detected from the samples of Permian-derived oils in TIC and *m*/*z* 177 mass chromatograms (Figures 10(c) and 10(f)), indicative of little secondary alteration. Therefore, these samples of crude oils and source rocks have complete distributions of *n*-alkanes, terpanes, and steranes in TIC, *m*/*z* 191, and *m*/*z* 217 mass chromatograms, respectively (Figures 10(c) 10(f), 10(i), and 10(l)). Considering that the oil seeps have slight biodegradation, we infer that biodegradation took place along the formation of oil seeps.

(4) Source of Oil Seeps. Samples of oil seeps in the SE and E have only suffered from lightly biodegradation as discussed above. As such, the molecular geochemical parameters of the seeps may have not been modified largely [26]. The overprinting of later charging of fresh oils may also do not disturb the oil-source determination of oil seeps as the oils are unbiodegraded and normal. Therefore, the molecular geochemical parameters with high fingerprint to organic facies may provide vital information to determine the source of oil seeps (Table 2; Figure 11; [26]).

As outlined above, there are two sets of possible source rocks in the study area including Permian lacustrine and Jurassic swamp-facies source rocks [31, 66]. Geochemical

characteristics of Jurassic-derived oils and source rocks have been discussed in detail above (see "(4) Source of oil seeps" section). Different from Jurassic-derived oils and source rocks, the middle Permian source rocks in the study area including Lucaogou (P_2l) and Pingdiquan (P_2p) formations have light carbon isotopic compositions ($\delta^{13}C_{VPDB}<-29‰$), low Pr/Ph values (1.0–2.0), high abundances of β-carotane and gammacerane (gammacerane/C_{30} hopane > 0.15), regular steranes that increase in abundance of the order C_{27}-C_{28}-C_{29}, and low abundances of diasteranes, indicating a reducing saline lacustrine facies [26, 31, 50]. Notably, geochemical characteristics of the Permian source rocks in the SE and E are somewhat similar to the Fengcheng source rocks in the NW (see discussion in "(4) Source of oil seeps" section for detail) but have lower abundances of β-carotane and gammacerane. They are somewhat similar to Paleogene and Cretaceous source rocks in the southern basin (see discussion in "(4) Source of oil seeps" and "(4) Source of oil seeps" sections for detail) but have lower abundances of diasteranes and different distribution of regular steranes C_{27}-C_{28}-C_{29}.

Based on these standards, the oil seeps in the SE and E are concluded to be derived from Permian source rocks (Figure 11; Table 2). In detail, the index characteristics include light $\delta^{13}C_{VPDB}$ values (−29.8‰ to −29.2‰; Figure 11(a); Table 2), high concentration of β-carotane evident in the TIC mass chromatograms (Figure 10(a)–10(c)), low values of C_{19}/C_{20} tricyclic terpanes (0.08–0.22) and C_{24} tetra-/C_{26} tricyclic terpanes (0.84–1.55; Figure 11(b); Table 2), low Ts/Tm values (0.10–0.21), high gammacerane index values (gammacerane/$C_{30}H = 0.22 – 0.29$) (Figure 11(d); Table 2), and high C_{29}/C_{30} hopanes (0.61–0.68) (Figure 11(e); Table 2) as evidenced in the m/z 191 mass chromatogram. These characteristics also include the regular steranes that increase in abundance in the order C_{27}-C_{28}-C_{29} (Figure 11(f); Table 2) and low concentrations of diasteranes (Dia/Reg = 0.18 – 0.21) (Figure 11(g); Table 2). The sterane isomerization index ($C_{29}\alpha\alpha\alpha$S/(S+R) and $C_{29}\alpha\beta\beta/(\alpha\beta\beta+\alpha\alpha\alpha)$) values of these oil seeps are 0.35–0.39 and 0.34–0.39, respectively (Figure 11(h); Table 2), indicating that all samples are of low maturity with similar maturities [61, 62].

In summary, we infer that the oil seeps in the SE and E were derived from Permian source rocks and are of low maturity in general.

5.3. Implications for Hybrid Petroleum Systems. Based on the results and discussion above, geochemical parameters of all the oil and gas seep samples that reflect unique organic facies are consistent with the crude oils and source rocks within each region (Figures 5, 7, 9, and 11; Table 2). As such, we infer that the genesis and distributional characteristics of the oil and gas seeps in the Junggar Basin are controlled by the source rocks from which these seeps are located. Therefore, we divide the oil and gas seeps in the Junggar Basin into five types. Typical compositions of each type, in terms of the stable and robust biomarkers and carbon isotopes, are shown in Table 3. The distributions of these five types of oil and gas seeps are shown in Figure 1(b). They represent different petroleum systems in spatial distribution. Because of the close relationship between oil and gas seeps and source rock, we can reveal the geochemical compositions of unknown source rocks by the study of oil and gas seeps in areas where there is a low research level or source-rock samples are lacking.

Oil and gas seeps represent the surface escapes of subsurface oil-gas reservoirs; therefore, they can be regarded as an indicator of migration or dysmigration of primary oil-gas reservoirs resulting in the formation of secondary hydrocarbon reservoirs ([1, 2]). As a result, generally, the spatial distribution of oil and seeps in the Junggar Basin is mainly within the structural zones along the junctional belts of basin-range systems characterized by active tectonics (Figure 1(b); [10, 45, 72, 73]).

In summary, the source of oil and gas seeps in the Junggar Basin is controlled by the development of source rocks, while the formation of the seeps are mainly controlled by tectonic activities [74, 75]. Thus, the invaluable geochemical data of oil and gas seeps present in this study, reflecting the process of secondary adjustment of hybrid petroleum systems, could promote the understanding of the systems in the Junggar Basin (Figure 13).

Figure 13 presents the scheme hybrid petroleum systems in the Junggar Basin. Based on the results and discussion in this study, boundary of secondary modification of petroleum systems was established and six potential zones T1–T6 for future exploration were proposed. The six areas can further be divided into two types. The first type includes T1–T3 zones, locating under the boundary of secondary modification, representing primary oil-gas reservoirs. For example, in the T2 area under Qigu outcrop, previous research reported Permian source rocks deposited here [25]. However, we have not detected the geochemical characteristics of this source rock within oil seeps in this study. Thus, we infer that oil-gas reservoirs derived from Permian source rocks might be located beyond the limitation of secondary adjustment.

The second type includes T4–T6 zones, laying above the boundary of secondary modification, and thus represents secondary oil-gas reservoirs. As such, the preservation conditions with high-quality regional caprocks are vital for their accumulation resulting in oil-gas reservoirs. For example, in the T4 zone under the Wuerhe outcrop, if effective caprocks are absent, the hydrocarbon reservoirs would be destroyed resulting in the formation of Wuerhe bitumen with severe biodegradation [45]. To the contrary, there would be secondary hydrocarbon adjustment resulting in secondary oil-gas reservoirs.

6. Conclusions

A wide range of oil and gas seeps occurs in the Junggar Basin, including bitumen, oil sand, crude-oil seep, and gas seep. The hydrocarbon seeps in different areas have distinct geochemical compositions, including in their carbon isotopic compositions, *n*-alkanes, isoprenoids (Pr and Ph), terpanes, and steranes, which are used to classify the oil and gas seeps into five types, which point to hybrid petroleum systems in the

Table 3: Genetic classification and geochemical characteristics of oil-gas seeps in the Junggar Basin.

Genetic types	Basic information				Typical molecular geochemical characteristics			
	Region	Formation	Oil source	Secondary alteration	$\delta^{13}C$ (‰; EOM)	Alkanes	Terpanes	Steranes
Type 1	NW	T_2k, K_1tg	P_1f	TIC: UCMs *m/z* 177: 25-norhopanes (severe biodegradation)	−28.90‰ to −27.50‰	*β*-Carotane (rich)	Ts/Tm = 0.04 – 0.05 $G/C_{30}H$ = 0.45 – 0.49	DRS: $C_{27}<C_{28}<C_{29}$; SII = 0.48 – 0.58 D/R = 0.20 – 0.25
Type 2	SE, E	P_2l (SE), J_1b (E)	P_2l/P_2p	TIC: UCMs (light biodegradation)	−29.80‰ to −29.20‰	*β*-Carotane (rich); Pr/Ph = 1.0	Ts/Tm = 0.10 – 0.21 $G/C_{30}H$ = 0.22 – 0.29	DRS: $C_{27}<C_{28}<C_{29}$; SII = 0.34 – 0.39 D/R = 0.18 – 0.21
Type 3	SM (Qigu)	J_3q	J	None	−28.30‰ to −27.80‰	*β*-Carotane (no); Pr/Ph = 1.80 – 2.40	$C_{19}T/C_{20}T$ = 1.07 – 1.16 $C_{24}Te/C_{26}T$ = 1.76 – 1.87 Ts/Tm = 0.67 – 0.69 $C_{29}/C_{30}H$ = 0.30 – 0.33 $G/C_{30}H$ = 0.12 – 0.13	DRS: $C_{27}<C_{28}<C_{29}$; SII = 0.52 – 0.56 D/R = 0.26 – 0.32
Type 4	SM (Anjihai and Huoerguosi)	$E_{2\text{-}3}a$	K	TIC: UCMs (light biodegradation)	−30.40‰ to −28.80‰	*β*-Carotane (high); Pr/Ph = 0.4 – 0.9	$C_{19}T/C_{20}T$ = 0.72 – 0.95 Ts/Tm = 1.09 – 1.64 $G/C_{30}H$ = 0.65 – 0.76	DRS: $C_{27}>C_{28}<C_{29}$; SII = 0.44 – 0.53 D/R = 0.37 – 0.48
Type 5	SW (oil seeps)	$E_{2\text{-}3}a$, N_2d	E (+J)	TIC: UCMs (light biodegradation)	−29.6‰ to −28.1‰	*β*-Carotane (rich); Pr/Ph = 1.2 – 1.3	$C_{24}Te/C_{26}T$ = 1.83 – 1.95 Ts/Tm = 0.64 – 0.98 $G/C_{30}H$ = 0.31 – 0.41	DRS: $C_{27}>C_{28}<C_{29}$; SII = 0.41 – 0.58 D/R = 0.33 – 0.41
	SW (gas seeps)	$E_{2\text{-}3}a$, N_2d	J	None	$\delta^{13}C_1$: −43.7‰ to −42.4‰ $\delta^{13}C_2$: −26.7‰ to −26.2‰	/	/	/

"/" denotes not applicable. Note: DRS = distribution of regular steranes; SII = sterane isomerization index; D/R = ratios of diasteranes to regular steranes.

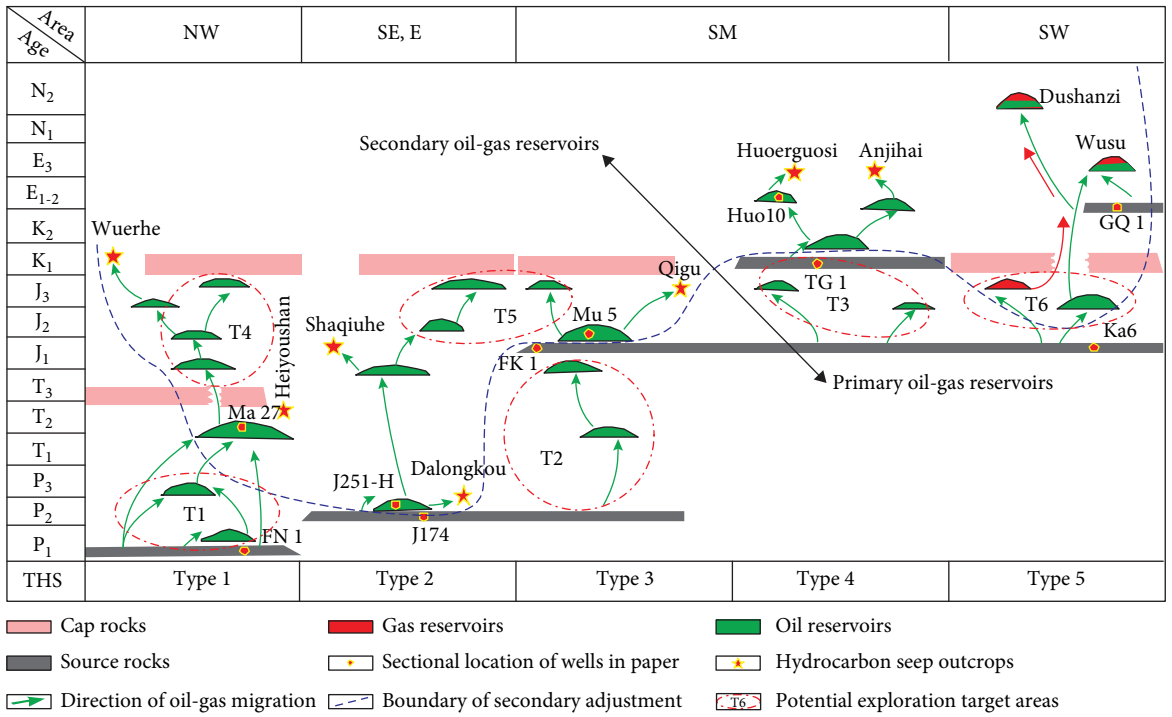

Figure 13: Genetic model of oil and gas seeps and its implications for hybrid petroleum systems of the Junggar Basin. THS: types of hydrocarbon seeps.

Junggar Basin. Six potential oil-gas exploration zones were proposed.

The gas seeps are derived from low-maturity Jurassic source rocks and occur in the Wusu and Dushanzi areas in the western segment of the southern basin. Type 1 oil seeps occur in the northwestern margin of the basin. They were derived from low Permian source rocks (P_1f) that were deposited in a hypersaline lacustrine setting. Type 2 oil seeps occur in the eastern margin and eastern segment of the southern margin of the basin. They originated from Permian source rocks that were deposited in a saline lacustrine setting. Type 3 oil seeps occur in the Qigu area in the central segment of the southern basin. They are derived from Jurassic swamp-facies rocks. Type 4 oil seeps occur in the Anjihai and Huoerguosi areas in the middle segment of the southern basin. They originated from Cretaceous source rocks that were deposited in a saline lacustrine setting. Type 5 oil seeps occur in the Wusu and Dushanzi areas in the western segment of the southern basin. They are originated mainly from Paleogene lacustrine rocks with some contribution from Jurassic rocks.

Data Availability

All data are available on request.

Conflicts of Interest

The authors declare that they have no conflicts of interest.

Acknowledgments

We thank Professor Mohamed Nady for detailed and constructive comments that greatly help to improve the paper. This work was jointly funded by the National Science and Technology Major Project of China (Grant No. 2016ZX05003-005), the PetroChina Science and Technology Major Project (Grant No. 2017E-0401), and the National Natural Science Foundation of China (Grant No. 41830425). We thank Wanyun Ma, Ji Li, and Julei Mi from PetroChina Xinjiang Oilfield Company for their kind assistance in the field work.

References

[1] S. Salati, F. J. A. van Ruitenbeek, E. J. M. Carranza, F. D. van der Meer, and M. H. Tangestani, "Conceptual modeling of onshore hydrocarbon seep occurrence in the Dezful embayment, SW Iran," *Marine and Petroleum Geology*, vol. 43, pp. 102–120, 2013.

[2] M. H. Tangestani and K. Validabadi, "Mineralogy and geochemistry of alteration induced by hydrocarbon seepage in an evaporite formation; a case study from the Zagros Fold Belt, SW Iran," *Applied Geochemistry*, vol. 41, pp. 189–195, 2014.

[3] J. B. Duan, Q. F. Zhang, and X. J. Fan, "Distribution of oil-gas seeps and characteristics of pool forming at Dabashan piedmont structural belt," *Geological Science and Technology Information*, vol. 35, pp. 163–167, 2016.

[4] G. A. Logan, A. T. Jones, J. M. Kennard, G. J. Ryan, and N. Rollet, "Australian offshore natural hydrocarbon seepage studies, a review and re-evaluation," *Marine and Petroleum Geology*, vol. 27, no. 1, pp. 26–45, 2010.

[5] J. X. He, Y. H. Zhu, J. N. Weng, and S. S. Cui, "Characters of north-west mud diapirs volcanoes in South China Sea and relationship between them and accumulation and migration of oil and gas," *Earth Science-Journal of China University of Geosciences*, vol. 35, pp. 75–86, 2010.

[6] Z. P. Huo, X. Q. Pang, Y. J. Du, W. B. Shen, T. Jiang, and F. T. Guo, "Oil-gas show from destruction oil/gas reservoirs in the petroliferous basin of China and their geological significance," *Oil & Gas Geology*, vol. 34, pp. 421–430, 2013.

[7] S. Sakran, M. Nabih, A. Henaish, and A. Ziko, "Structural regime and its impact on the mechanism and migration pathways of hydrocarbon seepage in the southern Gulf of Suez rift: an approach for finding new unexplored fault blocks," *Marine and Petroleum Geology*, vol. 71, pp. 55–75, 2016.

[8] J. Cao, Y. Zhang, W. Hu et al., "The Permian hybrid petroleum system in the northwest margin of the Junggar basin, Northwest China," *Marine and Petroleum Geology*, vol. 22, no. 3, pp. 331–349, 2005.

[9] Z. Jin, J. Cao, W. Hu et al., "Episodic petroleum fluid migration in fault zones of the northwestern Junggar Basin (Northwest China): evidence from hydrocarbon-bearing zoned calcite cement," *American Association of Petroleum Geologists Bulletin*, vol. 92, no. 9, pp. 1225–1243, 2008.

[10] G. Zheng, W. Xu, G. Etiope et al., "Hydrocarbon seeps in petroliferous basins in China: a first inventory," *Journal of Asian Earth Sciences*, vol. 151, pp. 269–284, 2018.

[11] PetroChina Xinjiang Oilfield Company, *The Distribution Rules of Oil–Gas Seeps in the Junggar Basin*, Internal Technical Reports, 1959.

[12] PetroChina Xinjiang Oilfield Company, *Oil–Gas Seeps Field Survey*, Internal Technical Reports, 1994.

[13] G. H. Fan and J. X. Li, "Discussion of oil-source in southern margin in Junggar Basin," *Xinjiang Petroleum Geology*, vol. 6, no. 4, pp. 11–18, 1985.

[14] Z. He, "Oil seepages in western segment of southern margin in Junggar Basin," *Xinjiang Petroleum Geology*, vol. 10, no. 1, pp. 87-88, 1989.

[15] J. X. Dai, X. Q. Wu, Y. Y. Ni et al., "Geochemical characteristics of natural gas from mud volcanoes in the southern Junggar Basin," *Science China Earth Sciences*, vol. 55, no. 3, pp. 355–367, 2012.

[16] H. L. Fan, C. K. Peng, X. Q. Yu et al., "Geochemical characteristics of Wusu mud volcanoes in Xinjiang and their mud sources," *Geological Bulletin of China*, vol. 36, pp. 1428–1438, 2017.

[17] Y. Gao, Y. L. Wang, and G. D. Zheng, "Geochemical characteristics of natural gas from Dushanzi mud volcano in Junggar Basin, Xinjiang," *Acta Geoscientica Sinica*, vol. 33, pp. 989–994, 2012.

[18] M. Li, D. D. Liu, and Z. J. Guo, "Geological characteristics of mud volcanoes and geochemical significance of the associated oil seepages in the southern Junggar Basin," *Geological Journal of China Universities*, vol. 19, pp. 484–490, 2012.

[19] X. X. Ma, G. D. Zheng, Z. F. Guo, G. Etiope, D. Fortin, and Y. Sano, "Estimation of greenhouse gas flux from mud volcanoes in the Dushanzi area, southern Junggar Basin of Northwest China," *Chinese Science Bulletin*, vol. 59, no. 32, pp. 3190–3196, 2014.

[20] G. Zheng, X. Ma, Z. Guo et al., "Gas geochemistry and methane emission from Dushanzi mud volcanoes in the southern Junggar Basin, NW China," *Journal of Asian Earth Sciences*, vol. 149, pp. 184–190, 2017.

[21] T. Abitkazy, J. H. Li, H. L. Li, W. B. Li, X. Mao, and H. H. Wang, "Tectonic evolution and hydrocarbon potential of basins in Central Asia and its adjacent regions," *Geoscience*, vol. 28, pp. 573–584, 2014.

[22] C. Z. Jia, B. L. Li, Y. L. Lei, and Z. X. Chen, "The structure of Circum-Tibetan Plateau Basin-Range System and the large gas provinces," *Science China Earth Sciences*, vol. 56, no. 11, pp. 1853–1863, 2013.

[23] F. J. Chen, X. W. Wang, and X. W. Wang, "Prototype and tectonic evolution of the Junggar basin, Northwestern China," *Earth Science Frontiers*, vol. 12, pp. 77–89, 2005.

[24] C. J. Zhang, D. F. He, X. Z. Wu et al., "Formation and Evolution of Multicycle Superimposed Basins in Junggar Basin," *China Petroleum Geology*, vol. 11, no. 1, pp. 47–58, 2006.

[25] J. P. Chen, X. L. Wang, C. P. Deng et al., "Geochemical features of source rocks and crude oil in the Junggar Basin, Northwest China," *Acta Geologica Sinica*, vol. 90, pp. 37–67, 2016.

[26] K. E. Peters, C. C. Walters, and J. M. Moldowan, *The Biomarker Guide: Second Edition II. Biomarkers and Isotopes in Petroleum Systems and Earth History*, Cambridge University Press, 2005.

[27] J. Dai, X. Xia, S. Qin, and J. Zhao, "Origins of partially reversed alkane $\delta^{13}C$ values for biogenic gases in China," *Organic Geochemistry*, vol. 35, no. 4, pp. 405–411, 2004.

[28] E. M. Galimov, "Isotope organic geochemistry," *Organic Geochemistry*, vol. 37, no. 10, pp. 1200–1262, 2006.

[29] R. L. Silva, C. A. M. Carlisle, and G. Wach, "A new TOC, rock-Eval, and carbon isotope record of lower Jurassic source rocks from the Slyne Basin, offshore Ireland," *Marine and Petroleum Geology*, vol. 86, pp. 499–511, 2017.

[30] J. X. Dai, S. F. Qin, S. Z. Tao, G. Y. Zhu, and J. K. Mi, "Developing trends of natural gas industry and the significant progress on natural gas geological theories in China," *Natural Gas Geoscience*, vol. 16, pp. 127–142, 2005.

[31] J. P. Chen, X. L. Wang, C. P. Deng et al., "Oil and gas source, occurrence and petroleum system in the Junggar Basin, Northwestern China," *Acta Geologica Sinica*, vol. 90, pp. 421–450, 2016.

[32] J. Chen, X. Wang, Y. Ni et al., "Genetic type and source of natural gas in the southern margin of Junggar Basin, NW China," *Petroleum Exploration and Development*, vol. 46, no. 3, pp. 482–495, 2019.

[33] P. A. Sun, B. L. Bian, Y. F. Yuan, X. Y. Zhang, and J. Cao, "Natural gas in southern Junggar Basin in Northwest China: geochemistry and origin," *Geochimica*, vol. 44, pp. 275–288, 2015.

[34] K. Tao, J. Cao, Y. Wang et al., "Geochemistry and origin of natural gas in the petroliferous Mahu sag, northwestern Junggar Basin, NW China: Carboniferous marine and Permian lacustrine gas systems," *Organic Geochemistry*, vol. 100, pp. 62–79, 2016.

[35] X. L. Wang, D. M. Zhi, Y. T. Wang et al., *Geochemistry of Source Rock and Petroleum in Junggar Basin*, Petroleum Industry Press, Beijing, 2013.

[36] J. P. Chen, C. P. Deng, X. L. Wang et al., "Formation mechanism of condensates, waxy and heavy oils in the southern margin of Junggar Basin, NW China," *Science China Earth Sciences*, vol. 60, no. 5, pp. 972–991, 2017.

[37] T. Bata, J. Parnell, S. Bowden, A. Boyce, and D. Leckie, "Origin of heavy oil in Cretaceous petroleum reservoirs," *Bulletin of Canadian Petroleum Geology*, vol. 64, no. 2, pp. 106–118, 2016.

[38] S. Larter, H. Huang, J. Adams et al., "The controls on the composition of biodegraded oils in the deep subsurface: part II – geological controls on subsurface biodegradation fluxes and constraints on reservoir-fluid property prediction," *Association of Petroleum Geologists Bulletin*, vol. 90, no. 6, pp. 921–938, 2006.

[39] S. R. Silverman, "Influence of petroleum origin and transformation on its distribution and redistribution in sedimentary rock," in *8th World Petroleum Congress*, pp. 47–54, Moscow, June 1971.

[40] J. K. Volkman, R. Alexander, R. I. Kagi, and G. W. Woodhouse, "Demethylated hopanes in crude oils and their applications in petroleum geochemistry," *Geochimica et Cosmochimica Acta*, vol. 47, no. 4, pp. 785–794, 1983.

[41] B. Bennett, M. Fustic, P. Farrimond, H. Huang, and S. R. Larter, "25-Norhopanes: formation during biodegradation of petroleum in the subsurface," *Organic Geochemistry*, vol. 37, no. 7, pp. 787–797, 2006.

[42] H. Huang and J. Li, "Molecular composition assessment of biodegradation influence at extreme levels—a case study from oilsand bitumen in the Junggar Basin, NW China," *Organic Geochemistry*, vol. 103, pp. 31–42, 2017.

[43] R. J. Hwang, S. C. Teerman, and R. M. Carlson, "Geochemical comparison of reservoir solid bitumens with diverse origins," *Organic Geochemistry*, vol. 29, no. 1-3, pp. 505–517, 1998.

[44] M. A. Rogers, J. D. Mcalary, and N. J. L. Bailey, "Significance of reservoir bitumens to thermal-maturation studies, Western Canada Basin," *AAPG Bulletin*, vol. 58, pp. 1806–1824, 1974.

[45] J. Zhang, J. Cao, Y. Wang, G. Hu, N. Zhou, and T. Shi, "Origin of giant vein-type bitumen deposits in the northwestern Junggar Basin, NW China: implications for fault-controlled hydrocarbon accumulation," *Journal of Asian Earth Sciences*, vol. 179, pp. 287–299, 2019.

[46] Y. Liu, K. Wu, X. Wang, B. Liu, J. Guo, and Y. du, "Architecture of buried reverse fault zone in the sedimentary basin: a case study from the Hong-Che fault zone of the Junggar Basin," *Journal of Structural Geology*, vol. 105, pp. 1–17, 2017.

[47] Z. S. Jiang and M. G. Fowler, "Carotenoid-derived alkanes in oils from northwestern China," *Organic Geochemistry*, vol. 10, no. 4-6, pp. 831–839, 1986.

[48] B. M. Didyk, B. R. T. Simoneit, S. C. Brassell, and G. Eglinton, "Organic geochemical indicators of palaeoenvironmental conditions of sedimentation," *Nature*, vol. 272, no. 5650, pp. 216–222, 1978.

[49] T. G. Powell and D. M. Mckirdy, "Relationship between ratio of pristane to phytane, crude oil composition and geological environment in Australia," *Nature Physical Science*, vol. 243, no. 124, pp. 37–39, 1973.

[50] L. M. Wenger and G. H. Isaksen, "Control of hydrocarbon seepage intensity on level of biodegradation in sea bottom sediments," *Organic Geochemistry*, vol. 33, no. 12, pp. 1277–1292, 2002.

[51] A. H. Knoll, R. E. Summons, J. R. Waldbauer, and J. E. Zumberge, "Chapter 8 -The geological succession of primary producers in the oceans," in *The Evolution of Primary Producers in the Sea*, P. Falkowski and A. H. Knoll, Eds., pp. 133–163, Academic Press, 2007.

[52] J. K. Volkman, S. M. Barrett, S. I. Blackburn, M. P. Mansour, E. L. Sikes, and F. Gelin, "Microalgal biomarkers: a review of recent research developments," *Organic Geochemistry*, vol. 29, no. 5-7, pp. 1163–1179, 1998.

[53] S. C. George, M. Lisk, and P. J. Eadington, "Fluid inclusion evidence for an early, marine-sourced oil charge prior to gas-condensate migration, Bayu-1, Timor Sea, Australia," *Marine and Petroleum Geology*, vol. 21, no. 9, pp. 1107–1128, 2004.

[54] A. D. Hanson, S. C. Zhang, J. M. Moldowan, D. G. Liang, and B. M. Zhang, "Molecular organic geochemistry of the Tarim Basin, Northwest China," *Association of Petroleum Geologists Bulletin*, vol. 84, pp. 1109–1128, 2000.

[55] R. P. Philp and T. D. Gilbert, "Biomarker distributions in Australian oils predominantly derived from terrigenous source material," *Organic Geochemistry*, vol. 10, no. 1-3, pp. 73–84, 1986.

[56] P. J. Grantham and L. L. Wakefield, "Variations in the sterane carbon number distributions of marine source rock derived crude oils through geological time," *Organic Geochemistry*, vol. 12, no. 1, pp. 61–73, 1988.

[57] W. Y. Huang and W. G. Meinschein, "Sterols as ecological indicators," *Geochimica et Cosmochimica Acta*, vol. 43, no. 5, pp. 739–745, 1979.

[58] J. K. Volkman, "A review of sterol markers for marine and terrigenous organic matter," *Organic Geochemistry*, vol. 9, no. 2, pp. 83–99, 1986.

[59] P. J. Grantham, "The occurrence of unusual C_{27} and C_{29} sterane prodominances in two types of Oman crude oil," *Organic Geochemistry*, vol. 9, no. 1, pp. 1–10, 1986.

[60] J. M. Moldowan, W. K. Seifert, and E. J. Gallegos, "Relationship between petroleum composition and depositional environment of petroleum source rocks," *AAPG Bulletin*, vol. 69, pp. 1255–1268, 1985.

[61] K. E. Peters and J. M. Moldowan, *The Biomarker Guide: Interpreting Molecular Fossils in Petroleum and Ancient Sediments*, Prentice Hall, Englewood Cliffs, NJ, USA, 1993.

[62] W. K. Seifert and J. M. Moldowan, "Applications of steranes, terpanes and monoaromatics to the maturation, migration and source of crude oils," *Geochimica et Cosmochimica Acta*, vol. 42, no. 1, pp. 77–95, 1978.

[63] B. Yang, Z. S. Jiang, J. X. Li, and W.,. X. L., *Oil Source of the Northwestern Margin of the Junggar Basin*, Gansu Science and Technology Press, Lanzhou, 1991.

[64] Z. Jiang and D. G. Fan, "Organic geochemistry of source rocks within Carboniferous Fengcheng Formation in Junggar Basin," *Xinjiang Petroleum Geology*, vol. 3, pp. 74–91, 1983.

[65] W. K. Seifert, J. M. Moldowan, and G. J. Demaison, "Source correlation of biodegraded oils," *Organic Geochemistry*, vol. 6, pp. 633–643, 1984.

[66] J. P. Chen, X. L. Wang, C. P. Deng et al., "Geochemical features and classification of crude oil in the southern margin of Junggar Basin, Northwestern China," *Acta Petrolei Sinica*, vol. 36, pp. 1315–1331, 2015.

[67] J. P. Chen, X. L. Wang, C. P. Deng et al., "Investigation of typical reservoirs and occurrence regularity of crude oils in the southern margin of Junggar Basin, Northwestern China," *Acta Petrolei Sinica*, vol. 37, pp. 415–429, 2016.

[68] J. P. Chen, X. L. Wang, C. P. Deng et al., "Oil-source of typical crude oils in the southern margin, Junggar Basin, Northwestern China," *Acta Petrolei Sinica*, vol. 37, pp. 160–171, 2016.

[69] M. M. el Nady, "Evaluation of the nature, origin and potentiality of the subsurface middle Jurassic and lower Cretaceous source rocks in Melleiha G-1x well, North Western Desert, Egypt," *Egyptian Journal of Petroleum*, vol. 24, no. 3, pp. 317–323, 2015.

[70] M. M. el Nady and N. S. Mohamed, "Source rock evaluation for hydrocarbon generation in Halal oilfield, southern Gulf of Suez, Egypt," *Egyptian Journal of Petroleum*, vol. 25, no. 3, pp. 383–389, 2016.

[71] R. L. Silva and L. V. Duarte, "Organic matter production and preservation in the Lusitanian Basin (Portugal) and Pliensbachian climatic hot snaps," *Global and Planetary Change*, vol. 131, pp. 24–34, 2015.

[72] Z. Wan, X. Wang, Y. Lu, Y. Sun, and B. Xia, "Geochemical characteristics of mud volcano fluids in the southern margin of the Junggar basin, NW China: implications for fluid origin and mud volcano formation mechanisms," *International Geology Review*, vol. 59, no. 13, pp. 1723–1735, 2017.

[73] J. K. Zhang, J. X. Zhou, H. J. Wang et al., "The discovery of light oil in the overlap-erosion zones of the northwestern Junggar Basin and its significance," *Geological Bulletin of China*, vol. 36, pp. 493–502, 2017.

[74] A. Mazzini and G. Etiope, "Mud volcanism: an updated review," *Earth-Science Reviews*, vol. 168, pp. 81–112, 2017.

[75] A. Mazzini, A. Nermoen, M. Krotkiewski, Y. Podladchikov, S. Planke, and H. Svensen, "Strike-slip faulting as a trigger mechanism for overpressure release through piercement structures. Implications for the Lusi mud volcano, Indonesia," *Marine and Petroleum Geology*, vol. 26, no. 9, pp. 1751–1765, 2009.

[76] W. Jiang, Y. Li, and Y. Xiong, "Source and thermal maturity of crude oils in the Junggar Basin in Northwest China determined from the concentration and distribution of diamondoids," *Organic Geochemistry*, vol. 128, pp. 148–160, 2019.

[77] P.'a. Sun, J. Cao, X. Wang et al., "Geochemistry and origins of natural gases in the southwestern Junggar basin, Northwest China," *Energy Exploration & Exploitation*, vol. 30, no. 5, pp. 707–725, 2012.

[78] J. X. Dai, "Identification and distinction of various alkane gases," *Science in China Series B-Chemistry*, vol. 35, pp. 185–193, 1992.